Title

FORMALDEHYDE PHOTOCHEMISTRY: APPEARANCE RATE, VIBRATIONAL RELAXATION, and ENERGY DISTRIBUTION OF THE CO PRODUCT

Author

Houston, Paul L.

Publication Date

1976-02-01

Submitted to Journal of Chemical Physics

LBL-4913
Preprint

FORMALDEHYDE PHOTOCHEMISTRY: APPEARANCE RATE, VIBRATIONAL RELAXATION, AND ENERGY DISTRIBUTION OF THE CO PRODUCT

Paul L. Houston and C. Bradley Moore

February 1976

Prepared for the U. S. Energy Research and Development Administration under Contract W-7405-ENG-48

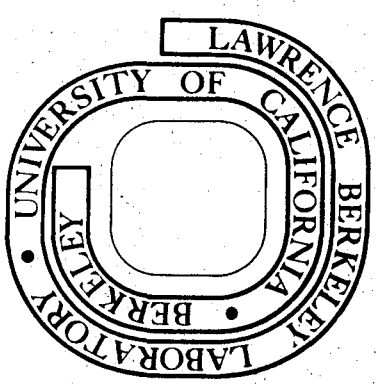

DISCLAIMER

LBL#4913

FORMALDEHYDE PHOTOCHEMISTRY: APPEARANCE RATE, VIBRATIONAL RELAXATION, AND ENERGY DISTRIBUTION OF THE CO PRODUCT

Paul L. Houston* and C. Bradley Moore
Department of Chemistry, University of California, Berkeley, California 94720

and

Materials and Molecular Research Division, Lawrence Berkeley Laboratory, University of California, Berkeley, California 94720

(Received)

The mechanism of formaldehyde photochemistry has been investigated by monitoring the appearance rate, relative yield, and vibrational distribution of the CO photochemical product detected either by its infrared fluorescence or by its absorption of a cw CO laser. In the limit of low formaldehyde pressures, the CO product appears with a rate more than 100 times slower than the decay rate of the formaldehyde first excited singlet state. This fact indicates the presence of a long-lived intermediate state between S_1 and the molecular

products. Collision-induced CO production following 337.1 nm formaldehyde excitation occurs with appearance rates of 2.7×10^{-11} cm^3 $molec^{-1}$ sec^{-1} for D_2CO and 4.7×10^{-11} cm^3 $molec^{-1}$ sec^{-1} for H_2CO. After its production, CO(v = 1) relaxes to the ground vibrational state in collisions with D_2CO at a rate of 3.3×10^{-12} cm^3 $molec^{-1}$ sec^{-1} and in collisions with H_2CO at a rate of 3.7×10^{-14} cm^3 $molec^{-1}$ sec^{-1}. These rates have been confirmed by a separate measurement which monitors CO(v = 1) fluorescence following excitation with a Q-switched CO laser. The CO photolysis yield decreases with the addition of argon, but increases dramatically for 305.5 nm photolysis upon the addition of NO or O_2. Vibrational distributions of the CO product have been measured as a function of energy and vibrational level of the formaldehyde singlet state. Although the amount of energy appearing in CO vibrational modes increases with increasing excitation energy, the CO vibrational energy accounts for only between 0.7 and 4.5% of the energy available to the products at the measured dissociation wavelengths.

I. INTRODUCTION

The photochemistry of formaldehyde has received an increasing amount of attention during the past five years for a variety of reasons. First, formaldehyde is the simplest of the aldehyde molecules. As such, an understanding of its photochemistry and of the nonradiative transitions which cause that photochemistry should aid considerably in our attempts to understand these processes in the higher aldehydes. Experimental studies of formaldehyde also form a basis for testing our current theories of nonradiative transitions. Since formaldehyde is found in interstellar space[1] and in polluted atmospheres,[2] there are a number of more practical applications of its photochemistry. Recently, the photochemistry of formaldehyde has also formed the basis for a separation process for hydrogen and carbon isotopes.[3-7]

Despite the large number of motivations for its study, it is only within the last six years that a general understanding for formaldehyde photochemistry has begun to emerge. McQuigg and Calvert[8] have demonstrated that the following processes are important:

$$H_2CO + h\nu \longrightarrow H_2CO(S_1, v') \quad (1)$$

$$H_2CO(S_1, v') \longrightarrow H_2 + CO \quad (2)$$

$$\longrightarrow H + HCO \quad (3)$$

$$\longrightarrow H_2CO(S_0, v'') + h\nu' \quad (4)$$

Following excitation (1), formaldehyde may dissociate into either molecular (2) or radical (3) products. There is also a small quantum yield for fluorescence (4). Generally, process (2) predominates for energies near the S_1 origin at 28,188 cm^{-1}, while process (3) predominates for energies above 32,250 cm^{-1}.[8]

Yeung and Moore[9] have measured collisionless lifetimes of H_2CO and D_2CO excited by a tunable ultraviolet laser source. The lifetimes of specific vibronic states decreases rapidly with increasing energy above the S_1 origin. Such studies have led to calculations of collisionless nonradiative lifetimes based on a model which assumes coupling between the originally excited singlet level and highly excited vibrational levels of the ground singlet state. These excited S_0 levels were expected to be broadened by rapid predissociation to molecular products, so that the dissociation mechanism may be represented by $S_1 \rightsquigarrow S_0 \longrightarrow H_2 + CO$. Calculations based on this model[10] are generally in good agreement with the reduction in lifetime as energy is increased above the S_1 origin and with the deuterium isotope effect. Despite this agreement, a number of questions still remain concerning the photodissociation pathway and dynamics.

One such question involves the possible role of the triplet state in formaldehyde dissociation. Miller and Lee[11] have argued that an alternative dissociation mechanism, $S_1 \rightsquigarrow T_1 \rightsquigarrow S_0 \longrightarrow H_2 + CO$, is also possible since appreciable yields of molecular products are observed from triplet benzene

sensitized decomposition of formaldehyde. Luntz and Maxson[12] have observed relatively short lifetimes of triplet formaldehyde following direct optical excitation with a tunable laser. They interpret these lifetimes to mean that $T_1 \rightsquigarrow S_0$ intersystem crossing is rapid and further conclude that collision-induced $S_1 \rightsquigarrow T_1$ crossing might also be important. An observation of the appearance rate for the molecular products might distinguish between the $S_1 \rightsquigarrow S_0 \longrightarrow H_2 + CO$ pathway and the $S_1 \rightsquigarrow T_1 \rightsquigarrow S_0 \longrightarrow H_2 + CO$ pathway. Assuming $S_0 \longrightarrow H_2 + CO$ to be fast, then in the former case CO should appear with the decay time of S_1, while in the latter case it should appear with the decay time of T_1.

A second question concerning the photodissociation of formaldehyde involves the distribution of energy among the molecular degrees of freedom of the products. Figure 1 shows the relevant energy-level diagram. The ground state of formaldehyde has very nearly the same energy as the $H_2(v = 0) + CO(v = 0)$ product channel, while the first excited formaldehyde singlet lies at 28,188 cm^{-1}. If dissociation takes place in the absence of collisions, then all of the S_1 energy is partitioned among the translation, rotation and vibration of the molecular products. Determination of the distribution of the energy among these various degrees of freedom might give some information about the S_0 surface in the region near the saddle point for dissociation. Furthermore, the relationship between the originally excited vibrational level of S_1 and the

vibrational distribution of the molecular products might yield information about the nonradiative couplings involved.

In order to investigate these questions, the present study is focused on the time-resolution and energy-distribution of the CO photochemical product. Appearance rates, relative yields, and vibrational distributions of the CO product have been measured using either absorption or fluorescence detection schemes following pulsed laser excitation of formaldehyde. The experimental apparatus which makes such an investigation possible is described in Section II. Section III describes measurements of vibrational relaxation of CO. Data on the CO photochemical product are presented in Section IV and discussed in Section V.

II. EXPERIMENTAL

The experiments of this study employed a number of individual excitation and detection components combined together to form configurations which provided information about the formaldehyde photochemistry. The individual excitation and detection components will be discussed in Section IIA, while their combination into three different experimental configurations will be described in Sections IIB, IIC, and IID.

A. Apparatus

There are two major requirements for any photochemical study: an excitation source for providing photons and a

detector for monitoring the formation of products. In order to measure the temporal behavior of CO formed following formaldehyde excitation, an ultraviolet pulse was needed whose duration was short compared to the dissociation process of interest and whose peak power was high enough to produce observable quantities of product. These requirements led to the selection of a laser as the excitation source.

Three ultraviolet lasers were used during this investigation. The first was a commercial nitrogen laser (Molectron, UV-1000) which emitted 6-10 mJ, 10 nsec pulses at a repetition rate of 25 Hz. The ultraviolet output of this laser consisted of a number of lines centered near 337.1 nm which overlap the formaldehyde absorption near the $2_0^1 4_0^1$ band[13] with an absorption coefficient of $\alpha \simeq 4 \times 10^{-4}$ cm^{-1} $torr^{-1}$. A second excitation source consisted of a Pockels cell Q-switched ruby laser doubled in a 2-inch length of KDP crystal to produce 50-100 mJ at 347.2 nm in a 10 nsec pulse. This laser has been described previously[9,14] as a component of a tunable ultraviolet laser system. In our study the 347.2 nm harmonic was used directly to excite formaldehyde to the 4_0^3 level of S_1. Although a large amount of excitation was obtained on each pulse, the low laser repetition rate of 0.05 Hz precluded effective signal averaging. The third excitation source was a commercial flashlamp-pumped dye laser (Chromatix, CMX-4) with intracavity doubling and narrowing accessories. This laser produced 1 μsec (FWHM) pulses at 30 Hz. The output

frequency could be tuned over most of the formaldehyde absorption spectrum from 270-350 nm, but for this study the laser was operated in the 294-317 nm region where the average pulse energy was roughly 0.2 mJ. Although the long pulse width of this laser made it difficult to study the appearance rate of the CO product, its tunability made it possible to measure CO product vibrational state distributions obtained from excitation at a variety of different formaldehyde absorption bands.

The second requirement for this study of formaldehyde photochemistry was a method for observing the CO photochemical product. Since the aim of this study was to monitor the relative amount of CO, its appearance rate and its vibrational distribution, a method was needed for monitoring the time-dependent behavior of the CO immediately following the excitation pulse. Two methods were used, each of which had a characteristic detection apparatus.

If any of the CO product from formaldehyde photolysis is produced in a vibrationally excited state, its infrared fluorescence may be used as a monitor of its time-dependent concentration. In this case the detection apparatus is simply a fast infrared detector. Detector elements were 3 x 10 mm of either Cu:Ge or Hg:Ge (SBRC) cooled to liquid helium temperature. Essential to the detection scheme was the use of a cooled (77 K) interference filter which reduced the background radiation but allowed CO fluorescence to pass to the detector. These detectors have been described in

greater detail elsewhere.[15] The time constant for the detector and amplifier combination was typically 180 nsec.

For either of the detection methods used in this study, signal averaging was employed to enhance the signal-to-noise ratio. Signal traces were digitized using a transient recorder (Biomation 8100, 2048 points, 10 nsec/point minimum) and averaged in hard-wired signal analyser (Northern 575).

In the second method of product detection, the CO was monitored by its time-dependent absorption of radiation from a CO laser. The CO laser was similar to that described by Djeu[16] with the following two exceptions. No xenon was necessary in order to obtain the $1 \rightarrow 0$ transistions, and Q-switched as well as cw operation was possible. A schematic diagram of the laser tube is shown in Fig. 2. The essential features which distinguish this laser are that the entire active length is cooled with liquid nitrogen and that CO diffusion to the unexcited regions at the ends of the tube is prevented by a double flow system. Pure helium entered the ends of the tube, while an $He/N_2/CO/air$ mixture entered at the electrodes. The flow of helium through the end sections helped to prevent back diffusion of the CO into the unexcited region where it would quench $1 \rightarrow 0$ laser action. The entire mixture was pumped out through the center of the tube by a 7 l/s mechanical pump connected to the laser through 4 m of 30 mm I.D. pyrex tubing. Typical operating pressures were 3 torr of helium from the outer ports and 1 torr of helium,

1 torr of N_2, and less than 0.1 torr of a mixture of 1% air in CO from the inner ports. Pressures were measured using an oil manometer connected at the laser outlet. Because of the presence of air in the discharge, some ozone was produced. As a precaution, all outlet tubing was made of glass or metal and a small amount of Ag foil was contained in the outlet tube to catalyze ozone decomposition.

When the laser was operated in the cw mode, the cavity was formed by a grating (Bausch and Lomb, 4μ, 300 lines/mm) and a 3-m radius-of-curvature output mirror coated for 98% reflection at 4.8μ (Coherent Radiation). A stabilization scheme was employed to lock the laser to the peak of the gain curve. The end mirror was modulated in position along the optical axis using a piezoelectric crystal (Burleigh, PZ-80), and the portion of the laser output from the zeroth order of the grating was detected with a PbSe detector (Optoelectronics). The signal from this detector, which is proportional to the slope of the gain curve, was monitored with a lock-in amplifier (PAR, HR-8) and used to position the laser at the peak of the gain curve. Under these conditions, the laser amplitude stability was better than 1%.

The cw laser operated typically with 1-2 mW of power on any one of 3 or 4 P-branch transitions near P(11) for each of the vibrational transitions $v \rightarrow v - 1$, where $v = 1,2,3,\ldots 10$. In the Q-switched mode of operation the grating was replaced by a rotating gold-coated mirror of 10-m radius curvature.

The laser then produced 1 μsec (FWHM) pulses at 100-200 Hz containing radiation from many vibration-rotation transitions. Of the total peak power of >2.5 kW, at least 300 W was produced on 1 → 0 transitions.

Gas handling was accomplished in a standard glass and grease vacuum system. Background pressures were typically $<10^{-6}$ torr and the leak rate was less than 1 mtorr/hr. Pressures were monitored either with a calibrated McLeod gauge or with a capacitance manometer (Celesco, P7D with CD-10 controler) calibrated against the McLeod gauge. Formaldehydes were prepared as described previously[9] and other gases were obtained from Matheson Co. with the following specified percent purities: Ar(99.9995), N_2(99.995), O_2(99.99), CO(99.99), NO(99.0, purified further by trap-to-trap distillation at - 131°C from traps containing glass wool).

The various excitation and detection components described above were combined to do three basic types of experiments. These three configurations are described in the following sections.

B. Photochemical Product Detection by CO Fluorescence

In this configuration either the nitrogen or dye laser excitation source was used to dissociate formaldehyde in a 10-cm long, 5-cm diameter quartz cell equipped with an NaCl window for observing infrared fluorescence. The excitation laser was passed 5 times through the quartz cell in

order to increase the signal-to-noise ratio. Carbon monoxide vibrational fluorescence was collected with a 2", f/1 NaCl lens, focused onto the element of one of the infrared detectors, and averaged for 1000-8000 laser shots. Fig. 3 shows an averaged fluorescence trace for a pressure of 5.29 torr of H_2CO excited by 1000 shots from the nitrogen laser. A single exponential decay was obtained. By expanding the timescale, the rise-time of the CO fluorescence could also be obtained.

In addition to the CO appearance and decay times, some measure of the vibrational distribution of the CO product is available from this experiment. The fact that fluorescence is observed at all indicates that CO is formed in $v \geq 1$. By interposing a 4 cm cell containing 5 torr of CO between the fluorescence cell and the detector, the fluorescence from CO($v = 1$) may be filtered from hitting the detector. Thus, the relative contributions of $v = 1$ and $v > 1$ may easily be obtained.

C. Photochemical Product Detection by CO Absorption

Although the experimental configuration outlined in the preceding section is capable of providing most of the desired information about the CO product, it does not give detailed information about the CO vibrational distribution. In particular, it tells nothing about CO($v = 0$) and is unable to distinguish among the levels with $v > 1$. In order

to overcome this difficulty, CO was also monitored by its time-dependent absorption of CO laser radiation. The experimental arrangement for this measurement is shown in Fig. 4.

The cw CO laser beam and any one of the pulsed ultraviolet laser beams were made to overlap spatially in a 1-m cell containing formaldehyde. The uv laser was collimated to a 5 mm diameter using a telescope of two quartz lenses and reflected into the cell by a mirror (M_1, Valpey) coated for 99% reflection in the near ultraviolet and 100% transmission in the infrared. The cw CO laser passed through mirror M_1, through the cell along a path defined by irises I_1 and I_2, and onto a detector (SBRC, Au:Ge, 77 K) with a 180 nsec response time. A mirror M_2, identical to M_1, and a piece of germanium, G_1, prevented the ultraviolet pulse from reaching the detector.

For an ultraviolet pulse of energy E in J, a formaldehyde absorption coefficient of α in cm^{-1} $torr^{-1}$, and a CO photochemical quantum yield of ϕ, it is possible to produce $E\alpha\phi$ x 1.8×10^{18} molecules of CO per cm of pathlength per torr of formaldehyde starting material, assuming a sample which is optically thin to the uv pulse. If the ultraviolet beam area is A in cm^2, then the partial pressure of CO produced in the beam per torr of formaldehyde starting material is

$$P_{CO} = E\alpha\phi A^{-1} \times 50 \text{ torr} \qquad (5)$$

For either the nitrogen laser or the tunable dye laser, P_{CO} is on the order of 0.1-1.0 m torr per torr of formaldehyde.

Roughly, 10^{-6} torr of CO per pulse could be detected with a signal-to-noise of unity after averaging.

The presence of CO in the path of the CO laser causes a change in the intensity of the infrared light hitting the detector which is given simply by Beer's Law. If the beam diameters of the two lasers are comparable, and if they overlap for a length ℓ, this change is

$$\frac{\Delta I}{I} \simeq 1 - \exp(- \alpha_{CO} P_{CO} \ell) \qquad (6)$$

where α_{CO} is the absorption coefficient for molecules whose vibrational state coincides with the lower CO laser level and it has been assumed that all of the CO molecules are produced in that state. For our experiments, α_{CO} is on the order of[17] 1.0 cm^{-1} $torr^{-1}$ and ℓ is 1 m so that the absolute magnitude of the argument of the exponent is always less than 0.1. Consequently, the error in assuming a linear proportionality of P_{CO} and ΔI is at most 5% and usually much less. Experimentally it was found that $\Delta I/I$ was always less than 0.1 and that the signal height was linear in all experimental variables (starting formaldehyde pressure and laser power) which might be related linearly to the CO pressure.

One further non-linearity may arise if signal averaging is used. Although Eq. (6) is valid for the first laser pulse, for CO(v = 0) measurements correction terms must be added for subsequent pulses due to the fact that there is a finite residual pressure of CO after CO from the previous pulses has

diffused to fill the cell. However, if the diameter of the cell is made much larger than the diameter of the beam, this effect may be minimized. For our experiments, the diameter of the cell was 76 mm while the diameter of the beam was $\sim$ 3 mm. Calculations show that for such an arrangement, many hundred shots may be averaged before correction terms become significant. In addition, it was experimentally verified that the intensity of the accumulated signal was linearly proportional to the number of shots averaged.

Figure 5 shows typical averaged signals for CO detection by the CO laser absorption technique. Figure 5(a) shows the signal obtained when the absorption was probed with a $2 \rightarrow 1$ vibrational laser transition, while Fig. 5(b) shows the result of absorption on a $1 \rightarrow 0$ transition. In both cases the nitrogen laser was used to dissociate H_2CO. If it is assumed that no CO was produced in $v \geq 2$, then Fig. 5(a) may be interpreted as simply a rise in absorption due to production of CO($v = 1$) followed by a decay due to vibrational relaxation. The signal in Fig. 5(b) then monitors the difference between molecules in $v = 0$ and $v = 1$. Initially, more molecules are produced in $v = 0$ than in $v = 1$, so that a rapid increase in absorption is observed. This rapid increase gives the appearance time for the CO product. On the 200 μsec timescale, CO($v = 1$) molecules are vibrationally relaxed to $v = 0$, so that the absorption of the $1 \rightarrow 0$ CO laser increases further during this period. Finally, on the 3 msec timescale, the CO molecules diffuse out of the probe beam and

the absorption disappears.

Using this method of detection, CO vibrational distributions and relative yields as well as CO appearance and decay rates could be measured.

D. Apparatus for CO Relaxation Measurements.

The decay curves of Fig. 3 and Fig. 5(a) may be interpreted as vibrational relaxation of CO(v = 1) by formaldehyde. In order to test this assumption and in order to test our understanding of the CO detection signals following formaldehyde dissociation, it was found desirable to have an independent measurement of the vibrational relaxation of CO by formaldehyde. This section describes the experimental configuration for such a measurement using the technique of laser-induced vibrational fluorescence.[18]

The CO laser was used in its Q-switched mode of operation to excite CO to v = 1 in a fluorescence cell formed of a pyrex "T", 6.5 cm long by 2 cm in diameter. The laser beam entered the cell through a salt window, struck a gold-coated mirror at the rear end of the cell, and was reflected back along its incoming direction. Vibrational fluorescence was observed at right angles to the beam through a second salt window. Typically, varying pressures of formaldehyde were added to a mixture of 50 mtorr of CO in 40 torr of argon. The argon was necessary to keep the temperature rise in the beam to less than 1 K following the infrared excitation pulse.

The fact that the laser pulse contains radiation from many other rotation-vibration transitions in addition to the $1 \rightarrow 0$ transitions causes two potential problems. The first problem is that it is difficult to prevent scattered light from reaching the detector element, Cu:Ge in this case. This difficulty was overcome by the use of a cooled (77 K) circular variable interference filter (OCLI) positioned to pass fluorescence only on the CO $1 \rightarrow 0$ R-branch. The second potential problem is that the presence of $2 \rightarrow 1$ radiation may excite $v = 1$ molecules to $v = 2$, in which case the fluorescence decay would be a measure not only of $v = 1$ deactivation but also of $v = 2$ relaxation. By using a CO gas filter in addition to the circular variable filter, it was found that under our experimental conditions CO($v = 2$) fluorescence contributed less than 5% to the total fluorescence.

A typical averaged fluorescence trace is shown in Fig. 6 for a mixture of 54 m torr of CO, 41.5 torr of argon and 6.06 torr of H_2CO. Fluorescence decayed with a single exponential for nearly two orders of magnitude in intensity. Such traces were used to determine the relaxation of CO($v = 1$) and to facilitate a comparison of this rate to the CO deactivation observed following formaldehyde dissociation. The results are discussed in the following section.

III. VIBRATIONAL RELAXATION OF CO

Vibrational relaxation of CO by formaldehyde has been studied using three different techniques which yield identical results. In the first technique, CO(v = 1) was produced from photolysis of formaldehyde in the apparatus of Section IIB. Its fluorescence decay was then monitored as a function of the original formaldehyde pressure. The second technique was similar to the first, except that the decay of CO(v = 1) was monitored by the change in absorption of the 2 → 1 cw CO laser line as described in Section IIC. Finally, in the third technique, the Q-switched CO laser was used to excite CO as described in Section IID. CO vibrational fluorescence was then monitored as a function of added H_2CO, D_2CO, or HDCO.

The rates for deactivation of CO by H_2CO measured by the first and third techniques are shown in Fig. 7. Inverse deactivation times are plotted against the partial pressure of H_2CO. The circles are for fluorescence detection following dissociation of H_2CO by the nitrogen laser, while the triangles are for fluorescence detection following CO excitation with the Q-switched CO laser. The two types of measurements agree with one another to give a relaxation rate of $1.31 \pm .11 \times 10^3$ sec^{-1} $torr^{-1}$, as measured by the slope of the line in Fig. 7.

A similar plot for D_2CO deactivation of CO is shown in Fig. 8. For this plot, the second and third measurement

methods are compared. The circles are for the decay of the CO(v = 1) absorption signal following dissociation of D_2CO by the nitrogen laser, while the triangles again depict fluorescence decay following CO excitation by the Q-switched CO laser. A linear relationship is found whose slope yields a rate of $1.15 \pm .10 \times 10^5$ sec^{-1} $torr^{-1}$ for the deactivation of CO(v = 1) by D_2CO.

Deactivation of CO(v = 1) by HDCO is also shown in Fig. 8. The solid squares give reciprocal relaxation times as a function of HDCO pressure as obtained from the Q-switched laser excited fluorescence method. The slope of the line gives a rate of $6.5 \pm .7 \times 10^4$ sec^{-1} $torr^{-1}$ for the deactivation of CO(v = 1) by HDCO.

The results of these measurements are summarized in Table I. It should be noted that the deuterated formaldehydes relax CO(v = 1) nearly two orders of magnitude faster than does H_2CO. This enhancement of the relaxation rate is probably due to near-resonant vibration-to-vibration energy transfer. For H_2CO, none of the fundamental modes of vibration lies within 400 cm^{-1} of the CO fundamental at 2143 cm^{-1}. On the other hand, for D_2CO and HDCO, the ν_5 asymmetric stretch modes lie only $\sim$20 cm^{-1} from the CO(v = 1) level.[19] Consequently, the following collisions are likely to cause rapid deactivation of CO(v = 1):

$$CO(v = 1) + D_2CO(\nu_5 = 0) \longrightarrow CO(v = 0) + D_2CO(\nu_5 = 1) \quad -17\ cm^{-1} \qquad (7)$$

$$CO(v = 1) + HDCO(\nu_5 = 0) \longrightarrow CO(v = 0) + HDCO(\nu_5 = 1) + 23\ cm^{-1} \quad (8)$$

Similar near-resonant vibrational energy transfer has been observed previously for a variety of systems.[18]

Finally, the deactivation rates obtained from CO(v = 1) signals following formaldehyde dissociation and following Q-switched CO excitation are in excellent agreement. This fact strengthens the interpretation of the dissociation results presented in the following section.

IV. CO PHOTOCHEMICAL PRODUCT: RESULTS

A. Appearance Rate of the CO Product

The appearance rate of the CO product from 337.1 nm photolysis of either H_2CO or D_2CO was measured as a function of pressure by the absorption technique. Increase in absorption on either a 2 → 1 or a 1 → 0 CO laser transition typically exhibited a double exponential rise. In most cases the slower of these two rates for an i + 1 → i transition corresponded to relaxation of CO(v = i + 1) to CO(v = i), while the faster of the rates was assumed to correspond to the actual production of CO(v = i). However, the possibility of a second and slower production rate on the same timescale as the vibrational relaxation or on a longer timescale could not be entirely eliminated. The appearance rate was independent of the intensity of either laser over a factor of five

range in intensity and was also independent of the overlap geometry of the two beams.

Appearance rates varied linearly with pressure as shown in Fig. 9. Figure 9(a) shows the inverse appearance time as a function of pressure for photolysis of H_2CO at 337.1 nm. The triangles represent the appearance rate of CO(v = 1), while the squares represent the rate for CO(v = 0). The corresponding results for D_2CO are shown in Fig. 9(b). CO from either H_2CO or D_2CO was produced with a collisionless rate of less than 0.26 μsec^{-1} and a collision-induced rate given by the slope of the corresponding line in Fig. 9. These collision-induced rates are $k_{H_2CO} = 1.65 \pm .12\ \mu sec^{-1}\ torr^{-1}$ and $k_{D_2CO} = 0.96 \pm .07\ \mu sec^{-1}\ torr^{-1}$. For either H_2CO or D_2CO, the appearance rates for CO(v = 1) and CO(v = 0) were the same within experimental error.

An attempt was also made to measure the rate of CO appearance following H_2CO dissociation at 305.5 nm using the flashlamp-pumped dye laser and the absorption technique. Although the long (1 μsec) pulse duration of the excitation laser made it difficult to determine the appearance rate at higher pressures, at 0.15 torr this rate was less than 0.3 μsec^{-1}.

The effects of added argon and NO on the CO appearance rates following 337.1 nm excitation were also measured. In both cases CO was produced with a rate which increased with increasing pressure of the added gas. For 1.50 torr of

D_2CO and 0-15 torr of argon this appearance rate was given by $k_{Ar}^{D_2CO} = 0.10 \pm .01\ \mu sec^{-1}\ torr^{-1}$, while for 0.50 torr of H_2CO and 0-2 torr of NO the appearance rate was given by $k_{NO}^{H_2CO} = 1.9 \pm .5\ \mu sec^{-1}\ torr^{-1}$.

B. Relative Yield of the CO Product

The relative yield of CO was measured by both fluorescence and absorption detection methods as a function of laser intensity, formaldehyde pressure, and pressure of added foreign gas. For example, with the flashlamp pumped dye laser, the CO absorption signal for H_2CO dissociation was found to vary linearly between laser pulse energies of zero and 300 μJ. A linear relationship was also found between the CO absorption or fluorescence signals and the formaldehyde pressure as shown in Fig. 10 for fluorescence detection of CO produced by H_2CO photolysis at 337.1 nm. The zero-pressure intercept of the linear fit corresponds very closely to zero CO intensity. CO(v = 0) yields were also found to be linear in D_2CO pressure over the range 0-3 torr with zero intercept using the absorption technique.

The effect of added gases on the CO yield was also investigated. In addition to the possible kinetic effects of the added gas, two effects due to pressure broadening must be considered. The first is that pressure broadening may decrease formaldehyde absorption and, therefore, decrease the yield of product. However, for the uv absorption, the Doppler and Lorentz widths become equal only at ∿ 700 torr.

Consequently, measurements in the 0-15 torr range should be quite free from pressure broadening effects. Furthermore, since any of the uv excitation lasers is spectrally broad compared to the formaldehyde linewidth, absorption should not depend strongly on the linewidth even if broadening were present. The second effect of pressure broadening is more serious, however. For detection by the absorption technique, the absorption of the CO laser by the CO product is assumed to be independent of the pressure of added foreign gases. In reality, pressure broadening decreases the line-center CO absorption at a rate which depends on the ratio of the Lorentz to Doppler widths. For $a = \Delta\nu_L (\ln 2)^{1/2} / \Delta\nu_D$, the ratio of the broadened absorption coefficient to the unbroadened one is given in Appendix IX of Ref. 20. In the present case, absorption is at line center and $a = 0.017$ torr^{-1}, so that the absorption coefficient will be reduced by a factor[20] of about 1.5% per torr in the 0-15 torr range. The effects reported below for the addition of NO and O_2 gases are large enough so that correction for pressure broadening is unnecessary. For N_2 and argon, however, these corrections become important and have been incorporated into the analysis.

Figure 11 shows the relative change in the CO($v = 1$) absorption signal for addition of N_2, O_2, and NO to 2 torr of H_2CO photolyzed at 305.5 nm by the flashlamp pumped dye laser. The apparent decrease in the relative CO yield with added N_2 may be entirely attributed to the effects of pressure broadening as described above. However, it may be

easily seen from this figure that NO and O_2 produce a dramatically different effect from N_2. Similar effects were observed for all CO vibrational levels, although the magnitude of the effect for NO and O_2 depended somewhat on the particular vibrational level which was monitored. For example, the effect of O_2 was larger than that of NO for the production of CO(v = 0). The effect of NO on the CO(v = 1) absorption signal was found to decrease as the excitation energy approached the S_1 origin. At 326.0 nm the effect was about 60% of that at 305.5 nm, while at 337.1 nm the effect was barely noticeable.

The effect of argon on the CO(v = 0) absorption signal for dissociation of 1.5 torr of D_2CO at 337.1 nm was also measured. The CO yield in this case decreased roughly linearly over the range of 0-15 torr at a rate of 4% per torr. Of this decrease, 1.5% per torr may be attributed to the effect of pressure broadening on the CO absorption, assuming $\sigma_{CO\text{-}Ar} = 3.6$ Å.

C. Vibrational Distribution of the CO Product

The vibrational distribution of the CO photochemical product was measured as a function of energy and vibrational level of the formaldehyde first excited singlet state. Relative CO populations were derived by measuring the absorption of cw CO laser lines following formaldehyde dissociation. The apparatus described in Section IIC was employed. The CO laser was tuned to successively higher vibrational transitions until no signal was observed for

CO in vibrational states higher than some maximum v = vmax. If H_{v+1} denotes the signal height for absorption of the P(J), v + 1 → v laser line, then, in the harmonic oscillator approximation, the relative number density of CO in vibrational level v is given by

$$N_v - \frac{(2J+1)}{(2J-1)} N_{v+1} \sim H_{v+1}/(v+1) \tag{9a}$$

For v = vmax, $N_{v+1} = 0$ so that N_{vmax} is simply proportional to $H_{vmax+1}/(vmax+1)$. Solution of Eq.(9a) with this initial condition yields

$$N_v \sim \sum_{i=v}^{vmax} \left(\frac{2J+1}{2J-1} \right)^i H_{i+1}/(i+1) \tag{9b}$$

If there is a random percent error in measuring the signal heights of $\Delta H/H$, then the error in the fractional population of a vibrational level is given by

$$\Delta f_v \simeq 2 f_v (1 - f_v) (\Delta H/H) \tag{9c}$$

The reproducibility of the distributions measured by this method implied that $(\Delta H/H) \simeq 0.2$. In addition to this random error, the use of the harmonic oscillator approximation in Eq. (9a) incorporates a systematic error into the calculation of the distributions. However, the systematic error, which causes overestimation[21] of f_v by about 2.6% at v = 6, is much smaller than the random error and has been neglected.

The number densities obtained using this method give an accurate measurement of the relative populations provided that the signal height, H, is measured before any vibrational relaxation takes place. For the experiments reported here, the measured appearance rate of the CO product is always more than ten times faster than the observed rate for any of the CO vibrational deactivations. Consequently, it is quite easy to ensure that the measured distribution corresponds to that of the nascent CO photochemical product.

The results of such measurements are presented in Table II. The doubled ruby laser was used to obtain the results at 347.2 nm; the nitrogen laser was used for photolysis at 337.1 nm; and the tunable dye laser was used for all of the other bands. All distributions listed are for photolysis of 2 torr of H_2CO. Photolysis at 337.1 nm of D_2CO yielded the same CO distribution as photolysis of H_2CO within the experimental error. Within this same uncertainty, the distribution from 337.1 nm photolysis did not change as a function of pressure over the range of 0.5 - 3.0 torr.

For the photolysis at 337.1 nm, confirmation of the CO distribution is obtained from two further sources. Firstly, when the apparatus of Section IIB is used to detect CO fluorescence following dissociation of H_2CO by the nitrogen laser, >80% of the fluorescence is absorbed by the CO gas filter cell. This confirms that a smaller fraction of CO is produced in $v \geq 2$ than in $v = 1$ for photolysis at 337.1 nm.

Secondly, a method of partial analysis using the $1 \rightarrow 0$ absorption signal alone may be employed. Such a signal is shown in Fig. 5(b). While the initial difference in absorption is proportional to $N_0 - N_1$, the extrapolation of the long exponential decay back to the initial time yields a height which is proportional to $N_T = N_V$. Consequently, the $(N_0 - N_1)/N_T$ ratio may be obtained very simply from such a plot. This simple method of analysis yields $(N_0 - N_1)/N_T = 0.778$, while the more complicated method of Eq. (9b) yields $(N_0 - N_1)/N_T = 0.760$. These values agree to within the stated uncertainty (Eq. 9c).

V. CO PHOTOCHEMICAL PRODUCT: DISCUSSION

The CO photochemical product results of Section IV may be related simply if the following kinetic scheme is assumed:

$$I \xrightarrow{k^o_{m,i}} CO(v = i) + H_2 \qquad (10)$$

$$I \xrightarrow{k_{m,i}[F] + k^M_{m,i}[M]} CO(v = i) + H_2 \qquad (11)$$

$$I \xrightarrow{k^o_r} \text{products other than CO} \qquad (12a)$$

$$I \xrightarrow{k_r[F] + k^M_r[M]} \text{products other than CO} \qquad (12b)$$

In these equations, I is a state whose decomposition is the rate determining step in CO production. Equation (10)

represents a zero-pressure production of CO(v = i) while Eq. (11) represents collision-induced dissociation by formaldehyde, F, and foreign gases, M. Equations (12a) and (12b) are similar to Eqs. (10) and (11) with the exception that these rates take I to photochemical products other than CO, e.g. H + HCO or $H_2CO(S_0)$. Let

$$A = \sum(k^o_{m,i} + k_{m,i}[F] + k^M_{m,i}[M]) + (k^o_r + k_r[F] + k^M_r[M]) \quad (13)$$

and

$$B_i = k^o_{m,i} + k_{m,i}[F] + k^M_{m,i}[M] \quad (14)$$

where the summation is understood to be over the index i. Then it may be easily shown that the time dependence of I is given by

$$I(t) = I_o \exp(-At) \quad (15)$$

and the time dependence of CO(v = i) is given by

$$CO(v = i) = (B_i/A)\,[1 - \exp(-At)] \quad (16)$$

By using Eqs. (15) and (16), specific rate combinations may be identified with each of the results of Section IV. The appearance rate for CO in any vibrational state gives the same value, A; the relative yield of CO(v = i) at time zero gives B_i/A; and the distribution among the various vibrational levels gives the ratios B_i/B_j. The experimental results are discussed below in terms of this simple kinetic model. It must be stressed that this is not the only possible model.

A. Appearance Rate of the CO Product

The most important single conclusion from the present study is that formaldehyde does not dissociate directly from the first excited singlet state into the molecular products, but, rather, proceeds through some intermediate state. Baronavski and Moore[22] have recently reported the pressure dependence of the lifetimes for singlet formaldehydes excited at 337.1 nm. The zero-pressure lifetimes are $\tau_{D_2CO} \simeq 870$ nsec and $\tau_{H_2CO} \simeq 46$ nsec. At zero pressure the CO molecular product from either H_2CO or D_2CO is produced with an appearance time in excess of 4 μsec and possibly much longer. If the rate determining CO precursor, I, were the S_1 singlet state excited by the nitrogen laser, then, by Eqs. (15) and (16), CO should appear with the same rate, A, at which S_1 disappears. The fact that there is a delay in the appearance of CO indicates that there is at least one intermediate state in the dissociation path: $S_1 \rightsquigarrow I \longrightarrow CO + H_2$. Since the appearance rate for CO following H_2CO photolysis at 305.5 nm is also quite slow (less than 0.3 μsec^{-1}, Section IVA) and the decay of S_1 at this wavelength is expected[23] to be much faster than that at 337.1 nm, it seems likely that this intermediate also plays an important role for dissociation at higher energies.

An intermediate state is also important at pressures for which both S_1 is removed and CO is produced by collisions.

The rate of CO appearance for 337.1 nm excitation obeys Stern-Volmer kinetics for either H_2CO or D_2CO (Fig. 9): $k_{H_2CO} = 1.65 \pm .12$ μsec^{-1} $torr^{-1}$ and $k_{D_2CO} = 0.96 \pm .07$ μsec^{-1} $torr^{-1}$. The rate of S_1 decay is much faster and not linear with pressure.[22] The low pressure collision induced S_1 disappearance rates are $k_{H_2CO} \simeq 8$ μsec^{-1} $torr^{-1}$ and $k_{D_2CO} \simeq 1.5$ μsec^{-1} $torr^{-1}$. We conclude that neither collisionless nor collision-induced deactivation takes S_1 directly to molecular products.

The results of the CO appearance rate measurements (Section IVA) fit the kinetic scheme of Eqs. (10) - (12) with the following rate constants: $\Sigma k^o_{m,i} + k^o_r < 0.18$ μsec^{-1} and $\Sigma k_{m,i} + k_r = 0.96 \pm .07$ μsec^{-1} $torr^{-1}$ for D_2CO; and $\Sigma k^o_{m,i} + k^o_r < 0.26$ μsec^{-1} and $\Sigma k_{m,i} + k_r = 1.65 \pm .12$ μsec^{-1} $torr^{-1}$ for H_2CO. In addition, the rate constants for removal of I by NO and argon are given by $\Sigma k^M_{m,i} + k^M_r = 0.10 \pm 0.01$ μsec^{-1} $torr^{-1}$ for argon deactivating D_2CO and $k^M_{m,i} + k^M_r = 1.9 \pm 0.5$ μsec^{-1} $torr^{-1}$ for NO deactivating H_2CO (337.1 nm). For convenience, these rate constant summations have been summarized in Table III. A further identification of the components of the summations may be made using the distribution and yield results as shown below.

B. Relative Quantum Yield of the CO Product

Information on the relative quantum yield of the CO photolysis product may be used to further isolate many of the rate constants in Eqs. (10) - (12). For a fixed intensity and for the optically thin limit, the amount of light absorbed is linearly proportional to the pressure of formaldehyde. Therefore, the slope of a plot of CO signal intensity vs formaldehyde pressure is proportional to the CO quantum yield. The slope of Fig. 10 is independent of pressure. McQuigg and Calvert[8] have observed similar invariance of the molecular quantum yield, ϕ_m, with pressure in the range of 5-30 torr. The present study extends this range to 0.1 torr. An important consideration for comparison of our results with those of McQuigg and Calvert concerns the timescale on which the CO is produced. For our experiments, the observed CO comes directly from the photodissociation of formaldehyde to molecular products. Radical recombination processes at the concentrations present in our experiments can take place only on msec timescales where diffusion of the products out of the probe beam would obscure observation. In the study of McQuigg and Calvert, on the other hand, the final products of all possible reactions were observed and an estimation of the importance of radical recombination was obtained by measuring the extent of isotopic exchange following photolysis of H_2CO/D_2CO mixtures. Assuming that in our apparatus all the CO produced

by molecular dissociation is observed and that radical recombination is too slow to be observed, then the quantum yields reported by McQuigg and Calvert may be used to simplify the rate constant summations reported in Section VA.

In the high pressure limit, it may be seen from Fig. 9 that $(k_{m,i} + k_r)\,[F] >> k^o_{m,i} + k^o_r$. Therefore, for high pressures $\phi_m \equiv \Sigma B_i/A \simeq \Sigma k_{m,i}/(\Sigma k_{m,i} + k_r)$. The denominator of this last expression is known (Section VA, Table III). Taking the absolute quantum yields reported by McQuigg and Calvert,[8] $\phi_m = 0.79$ for H_2CO and $\phi_m = 0.35$ for D_2CO, then we find that $\Sigma k_{m,i} = 0.34 \pm .02$ μsec^{-1} $torr^{-1}$ and $k_r = 0.62 \pm .05$ μsec^{-1} $torr^{-1}$ for D_2CO; and $\Sigma k_{m,i} = 1.30 \pm .09$ μsec^{-1} $torr^{-1}$ and $k_r = 0.35 \pm .03$ μsec^{-1} $torr^{-1}$ for H_2CO. According to McQuigg and Calvert, the sum of the quantum yields for the molecular and radical paths is 1.0 for H_2CO and 0.39 for D_2CO. Thus, k_r takes I to radical products for H_2CO and to a combination of radicals (6%) and other products, e.g. $D_2CO(S_0)$, (94%) for D_2CO.

The effect of a foreign gas on the CO quantum yield using Eqs. (10) - (12) is given by

$$\frac{\text{Yield with M}}{\text{Yield without M}} = \frac{\Sigma k_{m,i}[F] + \Sigma k^M_{m,i}[M]}{(\Sigma k_{m,i} + k_r)[F] + (\Sigma k^M_{m,i} + k^M_r)[M]} \Big/ \frac{(\Sigma k_{m,i})}{(\Sigma k_{m,i} + k_r)} \qquad (17)$$

when [F] is large enough to neglect zero pressure rates. Argon decreases the yield of CO from D_2CO photolysis at 337.1 nm.

The rate constants involving [F], 1.5 torr of D_2CO in this case, have been separately measured, and the addition of argon yields $(\Sigma k_{m,i}^{Ar} + k_r^{Ar}) = 0.10 \pm .01$ μsec^{-1} $torr^{-1}$. The linear decrease in CO yield by 2.5% per torr argon (Section IVB) is well-matched by Eq. (17) when $k_r^{Ar} \simeq 9\ \Sigma k_{m,i}^{Ar}$; $k_r^{Ar} < 4\ \Sigma k_{m,i}^{Ar}$ gives a pressure dependence for the yield which is beyond the experimental error limits. In conclusion, it appears that quenching by argon takes D_2CO to products other than CO. The process may be deactivation of the intermediate to ground state formaldehyde.

The variation of CO yield from H_2CO dissociation as a function of added NO or O_2 pressure may also be interpreted using Eq. (17). The increase in appearance rate, at nearly constant CO yield, with increasing NO pressure at 337.1 nm (Section IVA and B) is reproduced by $(\Sigma k_{m,i}^{NO} + k_r^{NO}) = 1.9 \pm .5$ μsec^{-1} $torr^{-1}$ for $\Sigma k_{m,i}^{NO} \simeq 2k_r^{NO}$. At 305 nm McQuigg and Calvert[8] have found that the molecular quantum yield in pure H_2CO is 0.36 compared to 0.79 at 337 nm. The shape of the curves for O_2 and NO in Fig. 11 may be roughly reproduced by Eq. (17) if it is assumed that $\Sigma k_{m,i}^{NO,O_2}$ is about gas kinetic and much larger than k_r^{NO,O_2}. The large effect on CO yield at 305 nm compared to 337 nm results from the increase in H + HCO yield in pure H_2CO between 337 and 305 nm. In summary, the increase in CO yield with NO and O_2 pressure may be caused by collisions which take I mostly to CO + H_2 rather than to H + HCO. A possible alternative explanation that NO and O_2 react with HCO to produce CO[24] cannot be ruled out.

The possibility that NO or O_2 might prevent the formation of I by direct collisional quenching of S_1 to products may also be ruled out. At 305.5 nm, the wavelength for the results presented in Fig. 11, the zero pressure lifetime of S_1 is estimated to be about 1 nsec.[23] NO or O_2 would have to quench S_1 H_2CO with a rate greater than 100 times gas kinetic in order to compete with the spontaneous decay.

In conclusion, the experimental results for the relative CO yield are consistent with the mechanism proposed in Eqs. (10) - (12). However, more complicated schemes involving additional routes of radical production or subsequent radical reaction[24] paths may not be ruled out on the basis of our results. The rate constants deduced from the data using the proposed mechanism are summarized in Table III. They may be separated into contributions to each CO(v = i) channel using the vibrational distribution measurements as shown in the next section.

C. Vibrational Distribution of the CO Product.

Formaldehyde photolysis yields CO primarily in its ground vibrational state. Between 0.7 and 4.5% of the excess energy of a vibronic level of S_1 H_2CO above ground state H_2 + CO is found in vibration of the CO product (Table II). If energy were partitioned equally among the six internal degrees of freedom of H_2 and CO and the relative translation, each would receive 14%. As the vibrational energy of S_1 is increased, the fraction of energy going to CO product vibration increases. For example, excitation of the 4^3 level gives an average of 202 cm^{-1} vibrational excitation per CO, while excitation of $2^4 4^3$, 5100 cm^{-1} more energy in S_1, gives 1322 cm^{-1} in product CO vibration. The vibrational distribution of the CO product shown in Table II does not exhibit any dependence on the specific vibrational modes of H_2CO which are excited. Since the intermediate state has a lifetime of several collisions, this limited degree of correlation between specific S_1 excitation and CO product distribution is not surprising.

The measurement of the vibrational distribution from 337.1 nm photolysis allows separation of the sum of rate constants, $\Sigma k_{m,i}$, into the component parts by use of the equation

$$k_{m,i} = (\Sigma k_{m,i})\, f_i \qquad (18)$$

where f_i is the fraction of CO produced in state v = i from Table II.

D. Dissociation Mechanisms

The discovery of an intermediate state and the observation of some of its kinetic properties require a reevaluation of previously proposed mechanisms of formaldehyde molecular predissociation. The observations which any proposed mechanism must account for fall into three pressure regimes. At "high" pressures S_1 is collisionally quenched[9] to form I which is in turn destroyed by collisions to yield products. In an intermediate pressure range S_1 decays spontaneously[9,22] to I and I is again destroyed by collisions. At low pressures where neither S_1 nor I suffers collisions, there are no product studies. We know only that I is formed and that its zero pressure lifetime is longer than 5 μsec. It is possible that no H_2 + CO is produced in the absence of collisions. There is a great deal known about the decay of S_1 in the absence of collisions.[9] The S_1 lifetime decreases as its vibronic energy is increased, and the H_2CO lifetime is shorter than that for D_2CO. For collision-induced dissociation, any proposed mechanism must account for an increase in CO production upon addition of NO or O_2, and also must explain the large molecular yields from triplet benzene sensitized H_2CO decomposition.[11] Two mechanisms are discussed below.

Triplet Formaldehyde, $^3A_2$

One obvious candidate for the intermediate is the T_1 triplet state. Dissociation mechanisms for more complicated

systems such as acetaldehyde[26] and glyoxal[27,28] are known to proceed through triplet intermediates. A similar process might also occur in formaldehyde. For collision-induced dissociation, the triplet appears capable of explaining most of the experimental observations. Triplet benzene sensitization[11] could easily produce large concentrations of formaldehyde triplet which might then collisionally decompose to form molecular products. If the mechanism by which S_1 were converted to T_1 could maintain isotopic selectivity, and if triplet energy transfer were slow, then the triplet mechanism might account for the lack of isotopic scrambling[3-7] Collisional deactivation of $D_2CO(^3A_2)$ by NO is known[12] to be rapid with $k \simeq 3.7\ \mu sec^{-1}\ torr^{-1}$ so that the effect of NO and O_2 presented in Fig. 11 might easily be explained by the ability of these molecules to promote spin-orbit coupling. Such an interaction might preferentially couple the triplet to regions of the S_0 surface which produce molecules rather than radicals. The T_1 lifetime is also much shorter than that predicted from the integrated absorption coefficient[29] or from calculation;[30] thus, nonradiative decay processes such as $T_1 \rightsquigarrow S_0 \rightarrow D_2 + CO$ could govern the lifetime. A possible weak point of this proposal is that the self-quenching of $D_2CO(^3A_2)$ measured by Luntz and Maxson[12] for excitation near 390 nm and - 78°C is more than two orders of magnitude slower in rate than the collision-induced production of CO at 337 nm and room temperature ($0.96 \pm .07\ sec^{-1}\ torr^{-1}$, Fig. 9). The most important

drawback of the triplet model is the lack of a collisionless mechanism for triplet production.[9,10] Brand and Stevens[31] have extensively examined the formaldehyde spectrum for S_1 - T_1 perturbations. The sparsity of such perturbations and the sharp lines which result from those that occur indicate that it is extremely unlikely that the triplet, whose level density at the S_1 origin is only $\sim 0.02/cm^{-1}$, forms a dissipative manifold for S_1 collision-free decay. The triplet model, therefore, fails to provide an irreversible $S_1 \rightsquigarrow T_1$ decay channel at zero pressure or to explain the decrease in S_1 lifetime with increasing energy or H - D substitution.[9]

In conclusion, although the triplet offers attractive features in its candidacy for the observed intermediate, the absence of a mechanism for producing the triplet disqualifies it in the low and intermediate pressure ranges, while the disagreement of the $D_2CO(^3A_2)$ self-quenching rate with the CO appearance rate makes it unlikely in the intermediate and high pressure ranges.

Excited Vibrational Levels of S_0

Another candidate for the intermediate state is S_0 itself. Neither S_1 nor T_1 correlates directly with molecular products (Fig. 1), whereas S_0 correlates with both molecular and radical products. The S_0 state then presents itself as a natural intermediate in formaldehyde decomposition. Calculated $S_1 \rightsquigarrow S_0(v)$ intersystem crossing rates match the observed life-

time of S_1 fairly well.[10] While this agreement is based on the assumption of a rapid $S_0(v) \rightarrow H_2 + CO$ predissociation, in order for $S_0(v)$ to be the observed intermediate we must now suppose that these highly excited vibrational levels of the ground singlet are so weakly coupled to the continuum that they exist for many microseconds before dissociation.

In the collision-induced pressure regime we would then require deactivation of these high vibrational levels of S_0 to occur with rates which agree with those found for CO appearance. Triplet benzene sensitization[11] yields might then be explained by a $T_1 \rightsquigarrow S_0(v) \rightarrow H_2 + CO$ path. Isotopic selectivity[3-7] in the collision-induced regime could be maintained if the $S_1 \rightsquigarrow S_0(v)$ and $S_0(v) \rightarrow D_2 + CO$ processes were faster than the competing exchange mechanisms. Finally, the effect of NO and O_2 might be explained by a possible catalysis reaction of these molecules with $S_0(v)$ formaldehyde to give molecular products. By contrast, collisions with nitrogen must not show this effect. For the collision-induced pressure regime then, although agreement with the experimental observations requires much speculation, none of these observations rules out a mechanism involving a long-lived $S_0(v)$ intermediate.

For the collision-free regime, however, it is more difficult to reconcile such a mechanism with the observed phenomena. Under the present hypothesis, in contrast to the assumption of Ref. 10, the $S_0(v)$ intermediate state is long-

lived and, therefore, not appreciably broadened. For a long-lived S_0 to form a dissipative manifold for S_1 its level density must be greater than $2\pi c\tau$, where τ is the shorter of the S_1 and S_0 lifetimes. For measured values[9] of $\tau(S_1)$, this required density is much greater than that calculated for $H_2CO(S_0)$, about $10/cm^{-1}$ at the S_1 origin. While there is no evidence for much higher level densities, the possibility cannot be ruled out. Perhaps a geometry such as HCOH plays a role.

In summary, neither the triplet intermediate nor the $S_0(v)$ intermediate provides a convincing explanation for the available data. It seems likely that a combination of these and other processes, such as collision complexes, is involved. The mechanism may well change with excitation wavelength. Considerably more experimental and theoretical work will be required to establish a mechanism.

E. Dissociation Dynamics

If formaldehyde dissociates on the S_0 surface following a nonradiative transition from either S_1 or T_1, then the dissociation dynamics should be predicted by knowledge of the ground state formaldehyde surface and of the normal mode amplitudes and velocities at the geometry of the nonradiative transition. Potential surfaces for S_0, S_1 and T_1 have been calculated and examined for dissociation to either radical[32] or molecular[33] products. For the case of molecular dissocia-

tion on S_0, Jaffe et al.[33] have argued that, since the saddle point H - H and C - O distances are closer to the H_2CO values than to the H_2 and CO values, large vibrational excitation of the product molecules should be observed. However, it is clear from the results presented in Table II that only a small fraction (<5%) of the available energy is channeled into the CO vibrational mode. A closer examination of the potential surface[33] reveals that, while the C - O distance at the H_2CO dissociation saddle point corresponds to v = 1 or v = 2 for the free CO, the H - H distance at the saddlepoint corresponds to v = 4 in the free H_2. Therefore, it is possible that much of the available energy may be deposited in the H_2 vibration rather than in the CO vibration. Classical trajectory calculations on the surface calculated by Jaffe et al.[33] should provide a more accurate description of the possible final energy distributions.

VI. CONCLUSION

The present study has examined the mechanism of formaldehyde photochemistry by monitoring the relative quantum yield, appearance rate, relaxation, and vibrational distribution of the CO product. This product is formed primarily in its ground vibrational state (Table II). Kinetic results (Table III) show that formaldehyde does not dissociate to molecular products directly from the first excited singlet state, but, rather, proceeds through a long-lived intermediate. A

determination of the nature of this intermediate state requires much more theoretical and experimental examination. Theoretical investigations might focus on the height of the S_0 barrier to molecular dissociation, the extent of anharmonicity in and anharmonic couplings between high vibrational levels of S_0, and the vibrational product distributions predicted by classical trajectory studies on the S_0 surface. Direct spectroscopic observation of the intermediate state would be most valuable. It would also be extremely interesting to learn whether radical products, H + HCO, are produced from the same intermediate as is CO or whether they are created by an entirely different mechanism. The technique of time-resolved product detection presented here might easily be extended to investigation of the radical dissociation. It should be possible to monitor the H-atom product by its absorption and subsequent fluorescence of Lyman-α radiation. The HCO product might be monitored by its visible absorption.

ACKNOWLEDGMENTS

We are grateful to A. Baronavski, Y. Haas, W. Gelbart, K. Morokuma, and J. Jortner for many discussions of formaldehyde photochemistry. We also gratefully acknowledge the support of the National Science Foundation, the Army Research Office, Durham, and the Energy Research and Development Administration. Two of the lasers used in this study were purchased with a National Science Foundation grant for chemical instrumentation.

REFERENCES

*Present address: Department of Chemistry, Cornell University, Ithaca, New York 14853.

1. D.M. Rank, C.H. Townes, and W.J. Welch, Science 174, 1083 (1971).
2. R.S. Berry and P.A. Lehman, Ann. Rev. Phys. Chem. 22, 47 (1971).
3. E.S. Yeung and C.B. Moore, Appl. Phys. Lett. 21, 109 (1972).
4. V.S. Letokhov, Chem. Phys. Lett. 15, 221 (1972) and Sov. Quant. Electron. 2, 337 (1975).
5. J. Marling, Chem. Phys. Letters 34, 84 (1975).
6. H.M. Bazhin, G.I. Skubnevskaya, N.I. Sorokin, and Y.N. Molin, JETP Lett. 20, 18 (1974).
7. J.H. Clark, Y. Haas, P.L. Houston, and C.B. Moore, Chem. Phys. Lett. 35, 82 (1975).
8. R.D. McQuigg and J.G. Calvert, J. Am. Chem. Soc. 91, 1590 (1969).
9. E.S. Yeung and C.B. Moore, J. Chem. Phys. 58, 3988 (1973).
10. E.S. Yeung and C.B. Moore, J. Chem. Phys. 60, 2139 (1974).
11. R.G. Miller and E.K.C. Lee, Chem. Phys. Lett. 27, 475 (1974).
12. A.C. Luntz and V.T. Maxson, Chem. Phys. Lett. 26, 553 (1974).
13. A.P. Baronavski, Ph.D. Dissertation, U.C. Berkeley, 1975.
14. E.S. Yeung and C.B. Moore, J. Am. Chem. Soc. 93, 2059 (1971).
15. J. Finzi, Ph.D. Dissertation, U.C. Berkeley, 1975.
16. N. Djeu, Appl. Phys. Lett. 23, 309 (1973).

17. W.S. Benedict, R. Herman, G.E. Moore, and S. Silverman, Astrophys. J. 135, 277 (1962).

18. C.B. Moore, Adv. Chem. Phys. 23, 41 (1973).

19. V.A. Job, V. Sethuraman, and K.K. Innes, J. Mol. Spectrosc. 30, 365 (1969).

20. A.C.G. Mitchell and M.W. Zemansky, Resonance Radiation and Excited Atoms, Cambridge Univ. Press, 1971, p. 328.

21. L.A. Young and W.J. Eachus, J. Chem. Phys. 44, 4195 (1966).

22. A.P. Baronavski and C.B. Moore, to be published.

23. R.G. Miller and E.K.C. Lee, Chem. Phys. Lett. 33, 104 (1975).

24. J.F. McKellar and R.G.W. Norrish, Proc. Roy. Soc. 254, 147 (1960).

25. Y. Haas and C.B. Moore, private communication.

26. C.S. Parmenter and W.A. Noyes, Jr., J. Am. Chem. Soc. 85, 416 (1963).

27. C.S. Parmenter, J. Chem. Phys. 41, 658 (1964); L.G. Anderson, C.S. Parmenter and H.M. Poland, Chem. Phys. 1, 401 (1973).

28. J.T. Yardley, J. Chem. Phys. 56, 6192 (1972).

29. V.E. DiGiorgio and G.W. Robinson, J. Chem. Phys. 31, 1678 (1959).

30. T. Yonezawa, H. Kato, and H. Kato, J. Mol. Spectrosc. 24,500 (1967).

31. J.C.D. Brand and C.G. Stevens, J. Chem. Phys. 58, 3331 (1973).

32. D.M. Hayes and K. Morokuma, Chem. Phys. Lett. 12, 539 (1972).

33. R.L. Jaffe, D.M. Hayes, and K. Morokuma, J. Chem. Phys. 60, 5108 (1974).

TABLE I: Relaxation of CO(v = 1) by Formaldehydes

Relaxing Species	$k(sec^{-1}\ torr^{-1})$	Number of Collisions
H_2CO	$1.31 \pm .11 \times 10^3$	7340
HDCO	$6.5 \pm .7 \times 10^4$	148
D_2CO	$1.15 \pm .10 \times 10^5$	84

TABLE II: CO Vibrational Distributions

λ (nm)	H_2CO Vibrational level	Product CO Fraction v=0	1	2	3	4	5	6	Percent of Available E
347.2	4_0^3	.900	.100						0.7
337.1	$4_0^2 6_0^1$	.870	.110	.020					1.1
317.0	$2_0^2 4_0^3$	.731	.213	.049	.005	.002			2.3
314.5	$2_0^3 4_0^1$	.663	.195	.071	.032	.021	.012	.005	4.1
309.1	$2_0^1 5_0^1, 2_0^2 4_0^3 6_0^1$	.607	.265	.092	.029	.005	.002		3.7
305.5	$2_0^3 4_0^3$	.661	.242	.058	.026	.009	.004		3.2
303.6	$2_0^4 4_0^1$	.571	.262	.103	.037	.015	.008	.004	4.5
295.0	$2_0^4 4_0^3$	.598	.255	.094	.034	.014	.005		3.9
294.0	$2_0^5 4_0^1$	.609	.264	.099	.024	.004			3.5

TABLE III: Summary of Rate Constants for Formaldehyde Photochemistry at 3371 Å.

Rate Constant*	Rate (μsec^{-1} $torr^{-1}$)		Refer to Section
	H_2CO	D_2CO	
$\Sigma k^{o}_{m,i} + k^{o}_{r}$	<0.26	<0.18	IVA, VA, Fig. 9
$\Sigma k_{m,i} + k_{r}$	1.65 ± .12	0.96 ± .07	IVA, VA, Fig. 9
$\Sigma k_{m,i}$	1.30 ± .09	0.34 ± .02	VB
k_r	0.35 ± .03	0.62 ± .05	VB
$\Sigma k^{Ar}_{m,i} + k^{Ar}_{r}$		0.10 ± .01	IVA, VA
$\Sigma k^{Ar}_{m,i}$		∿0.01	VB
k^{Ar}_{r}		∿0.09	VB
$\Sigma k^{NO}_{m,i} + k^{NO}_{r}$	1.9 ± .5		IVA, VA
$\Sigma k^{NO}_{m,i}$	∿1.3		VB
k^{NO}_{r}	∿0.6		VB

*As defined by Eqns. (10)-(12).

Figure 1. Energy Level Diagram for Formaldehyde. The dashed lines show the correlations of bound states to continua. The barrier heights are unknown.

Figure 2. Schematic diagram of the CO laser tube.

Figure 3. CO fluorescence following dissociation of H_2CO at 337.1 nm. A formaldehyde pressure of 5.29 torr was used and the fluorescence was averaged over 1000 shots of the nitrogen laser.

Figure 4. Apparatus for detection of CO molecules by their absorption of a cw CO laser. See text for description.

Figure 5. Absorption of cw CO laser lines by CO produced from H_2CO dissociation at 337.1 nm. (a) Absorption of the $P_2(11)$ line using 3.33 torr of H_2CO. The trace is the average of 208 laser shots. (b) Absorption of the $P_1(12)$ laser line using 4.55 torr of H_2CO. The trace is the average of 102 laser shots.

Figure 6. CO fluorescence following excitation of CO to v = 1 by a Q-switched CO laser. The trace is the average of 3100 laser shots for a mixture of 54 mtorr of CO, 41.5 torr of argon, and 6.06 torr of H_2CO.

Figure 7. Vibrational Deactivation of CO by H_2CO. The circles are for fluorescence detection following dissociation of H_2CO at 337.1 nm. The triangles are for fluorescence detection following CO excitation with the Q-switched CO laser.

The slope gives a rate of $k = 1.31 \pm .11 \times 10^3$ sec^{-1} $torr^{-1}$.

Figure 8. Vibrational Deactivation of CO by D_2CO and HDCO. The circles are for the decay of the CO(v = 1) absorption signal following D_2CO dissociation at 337.1 nm. The triangles and squares are for fluorescence decay following CO excitation with the Q-switched CO laser in mixtures with D_2CO and HDCO, respectively.

Figure 9. Appearance Rate of the CO Product from H_2CO (a) and from D_2CO (b). In both cases dissociation was at 337.1 nm. The triangles represent the appearance rates for CO(v = 1), while the squares represent the appearance rates for CO(v = 0).

Figure 10. CO Fluorescence Intensity as a Function of H_2CO Pressure for dissociation at 337.1 nm.

Figure 11. CO(v = 1) Absorption Signal as a Function of Added Gas Pressure for Dissociation of H_2CO at 305.5 nm.

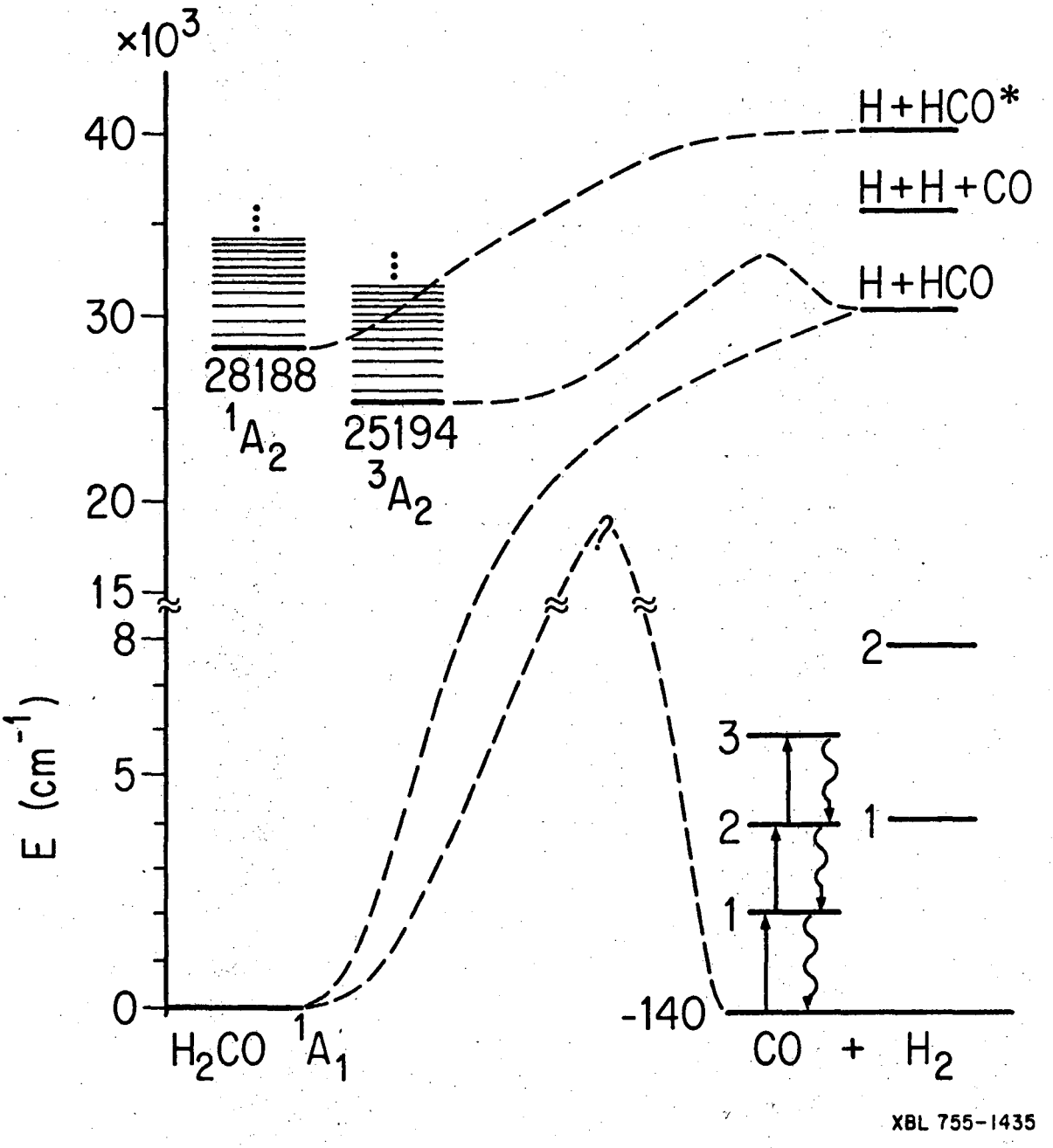

Fig. 1

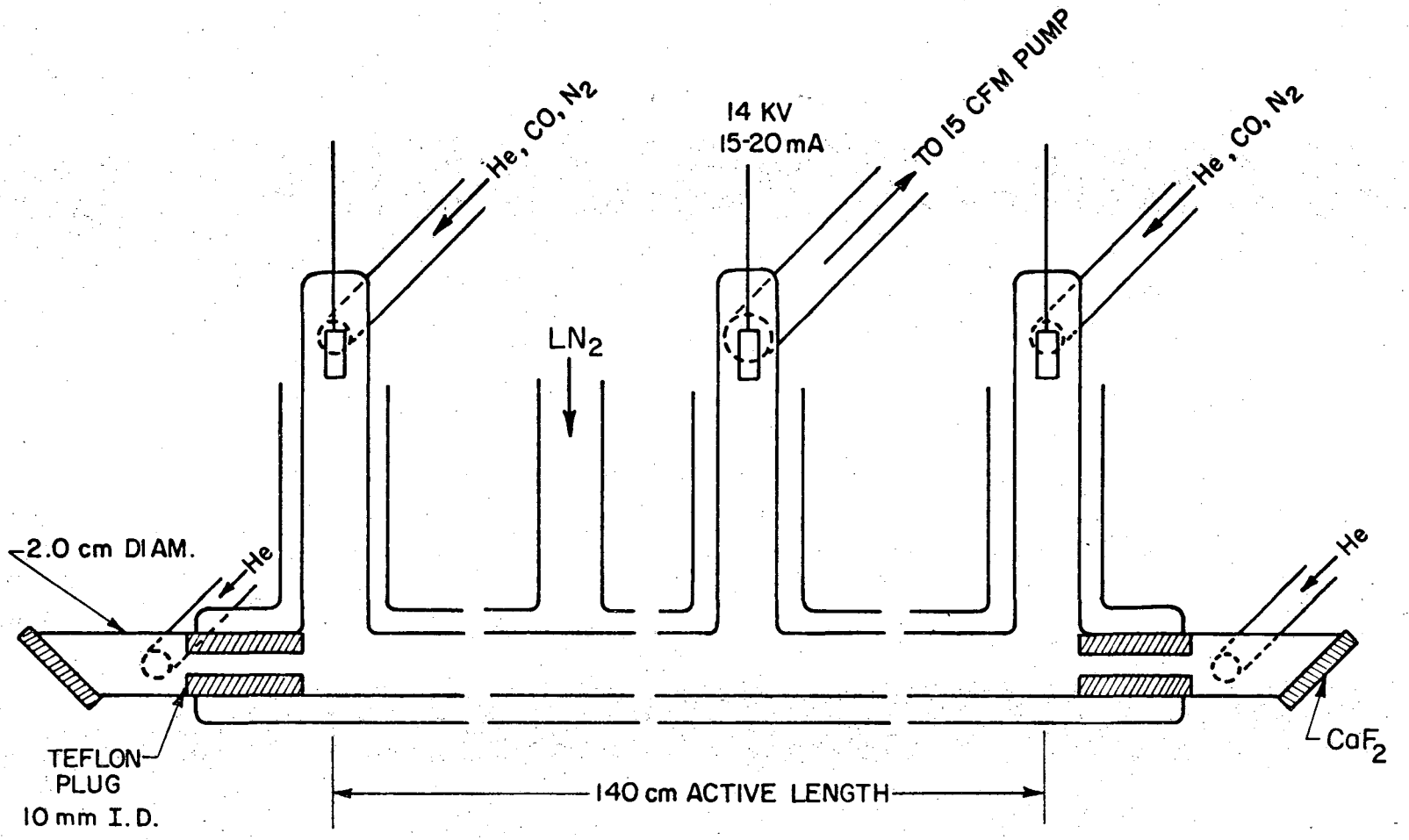

XBL 756-1489

Fig. 2

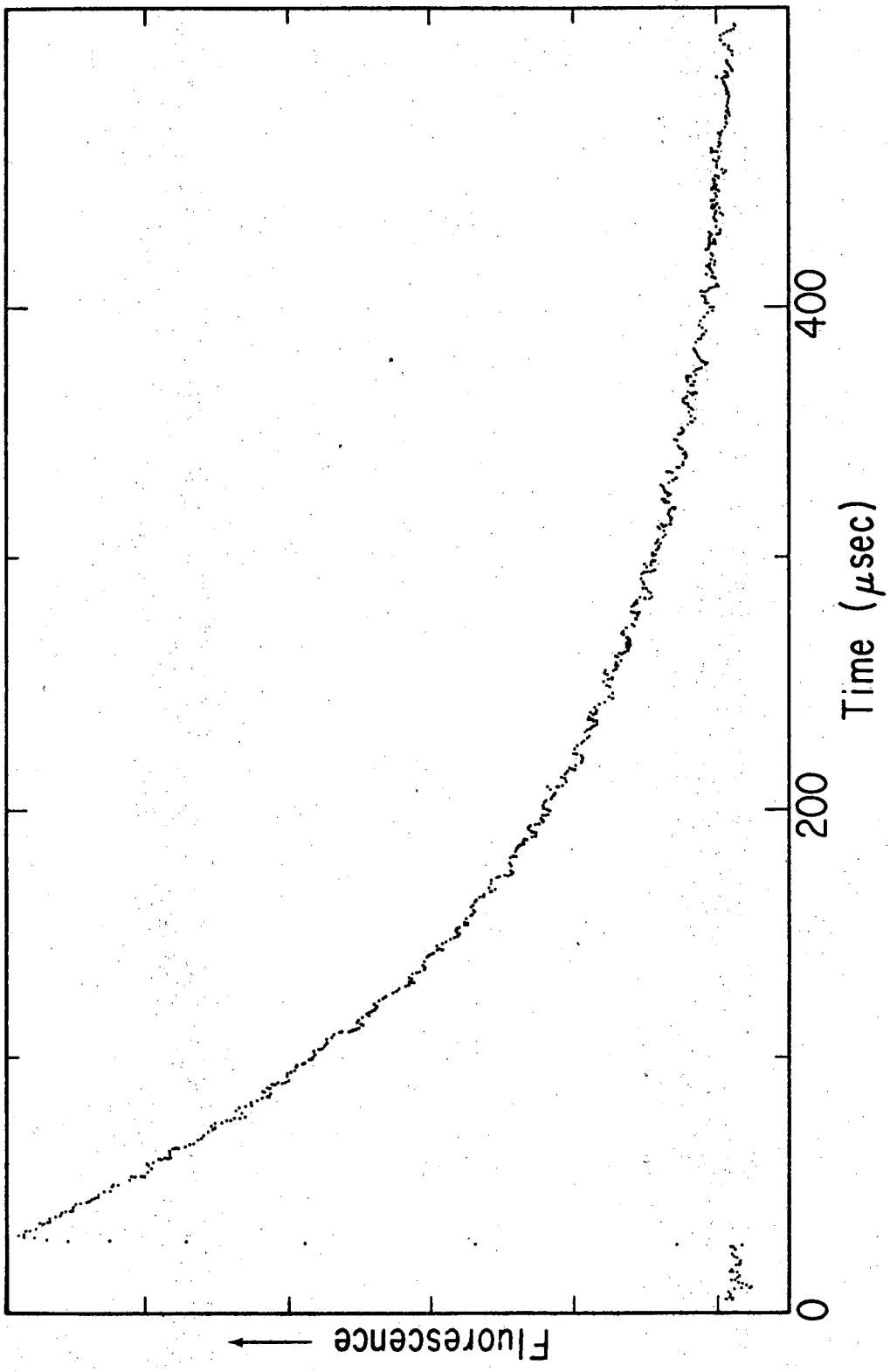

XBL 756-1490

Fig. 3

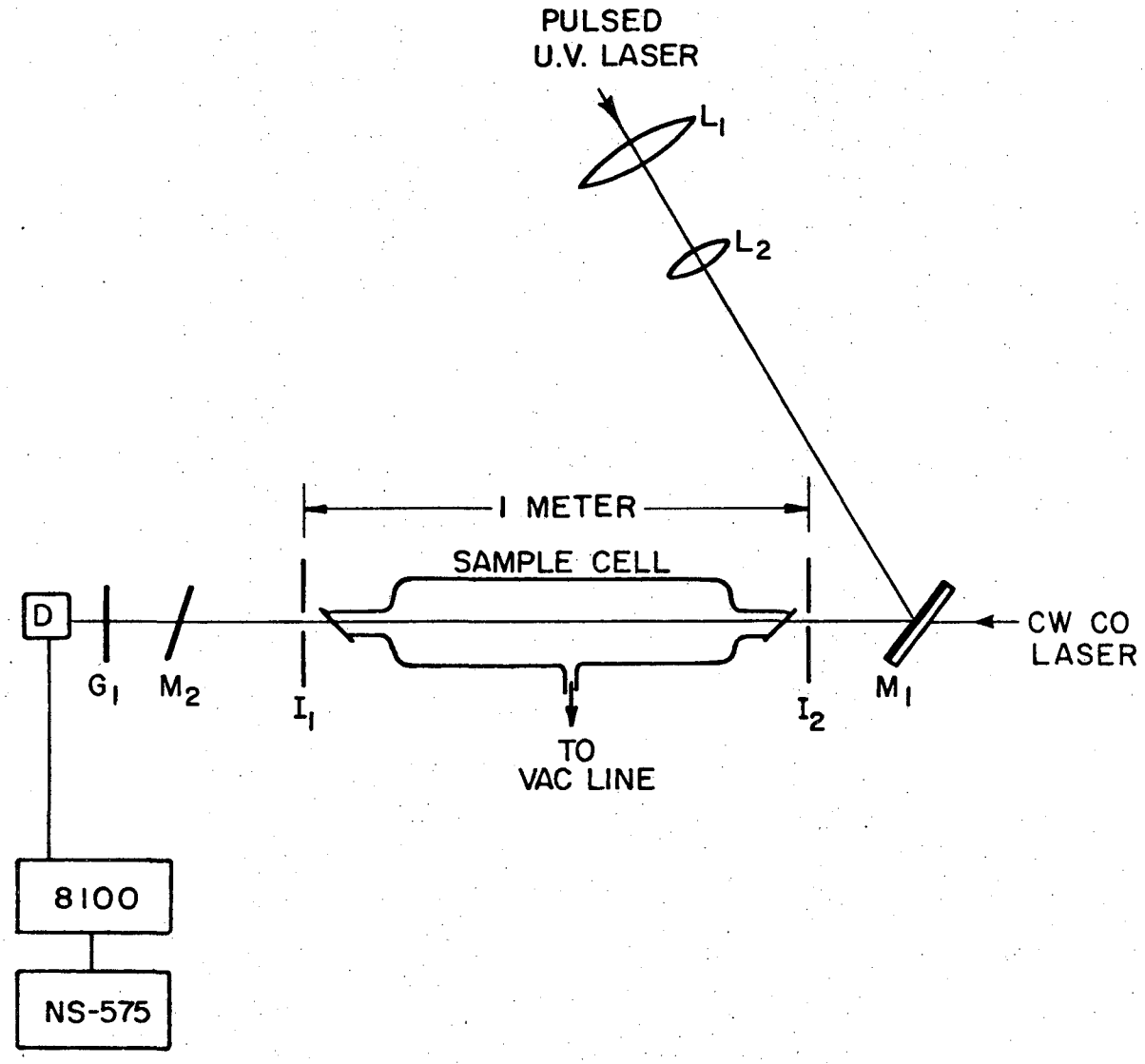

XBL 756-1488

Fig. 4

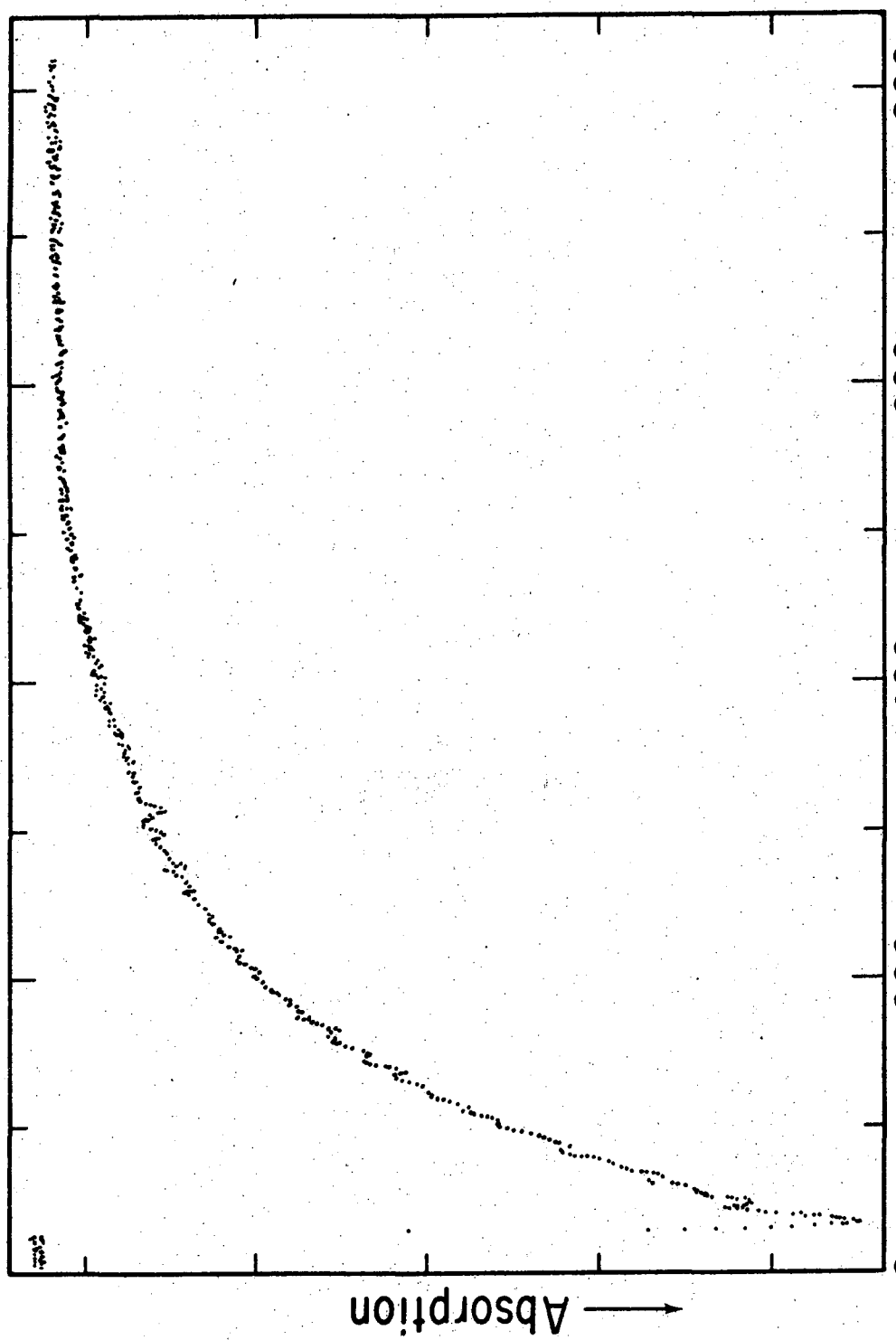

XBL 756-1491

Fig. 5a

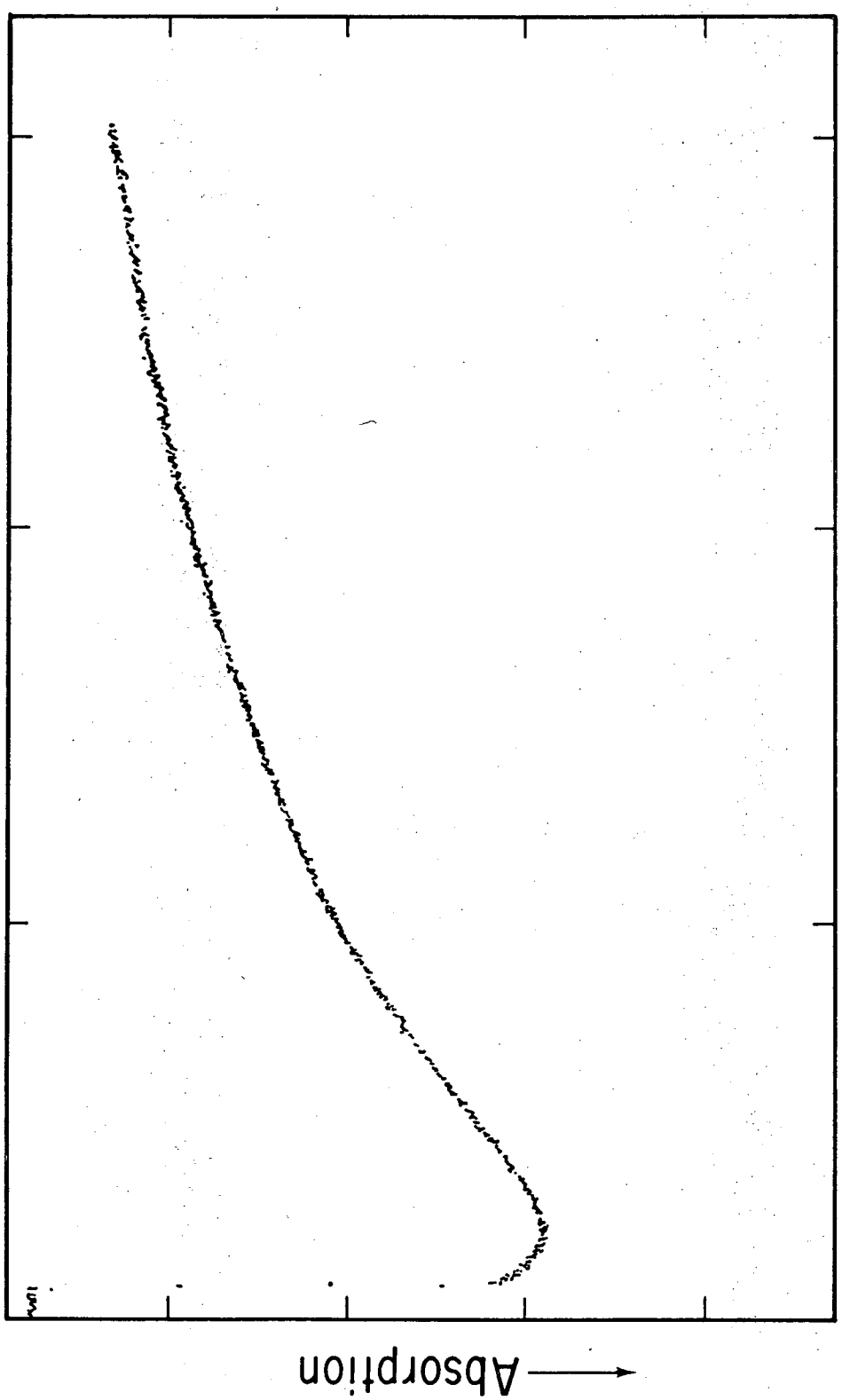

XBL 756-1492

Fig. 5b

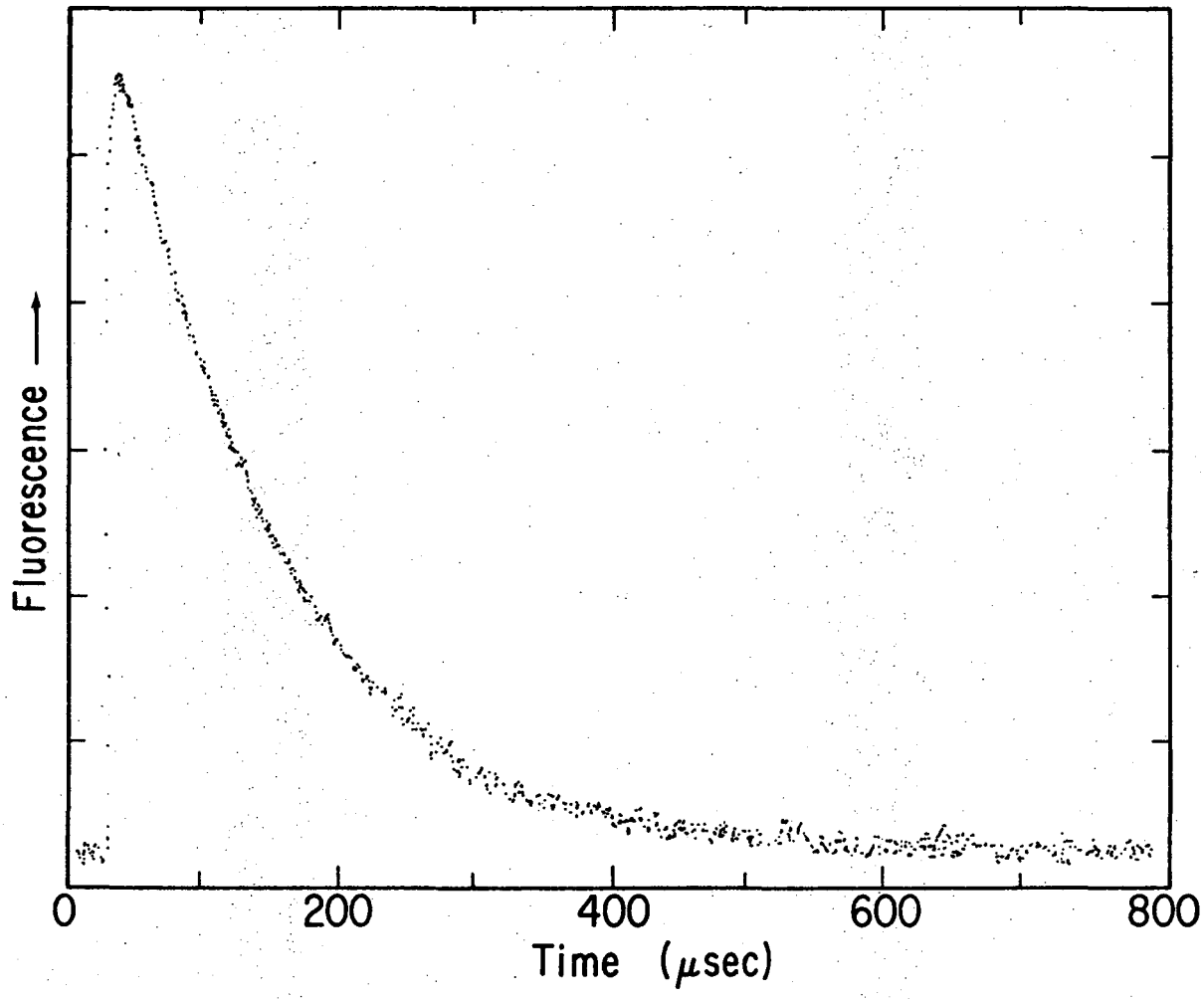

XBL 756-1486

Fig. 6

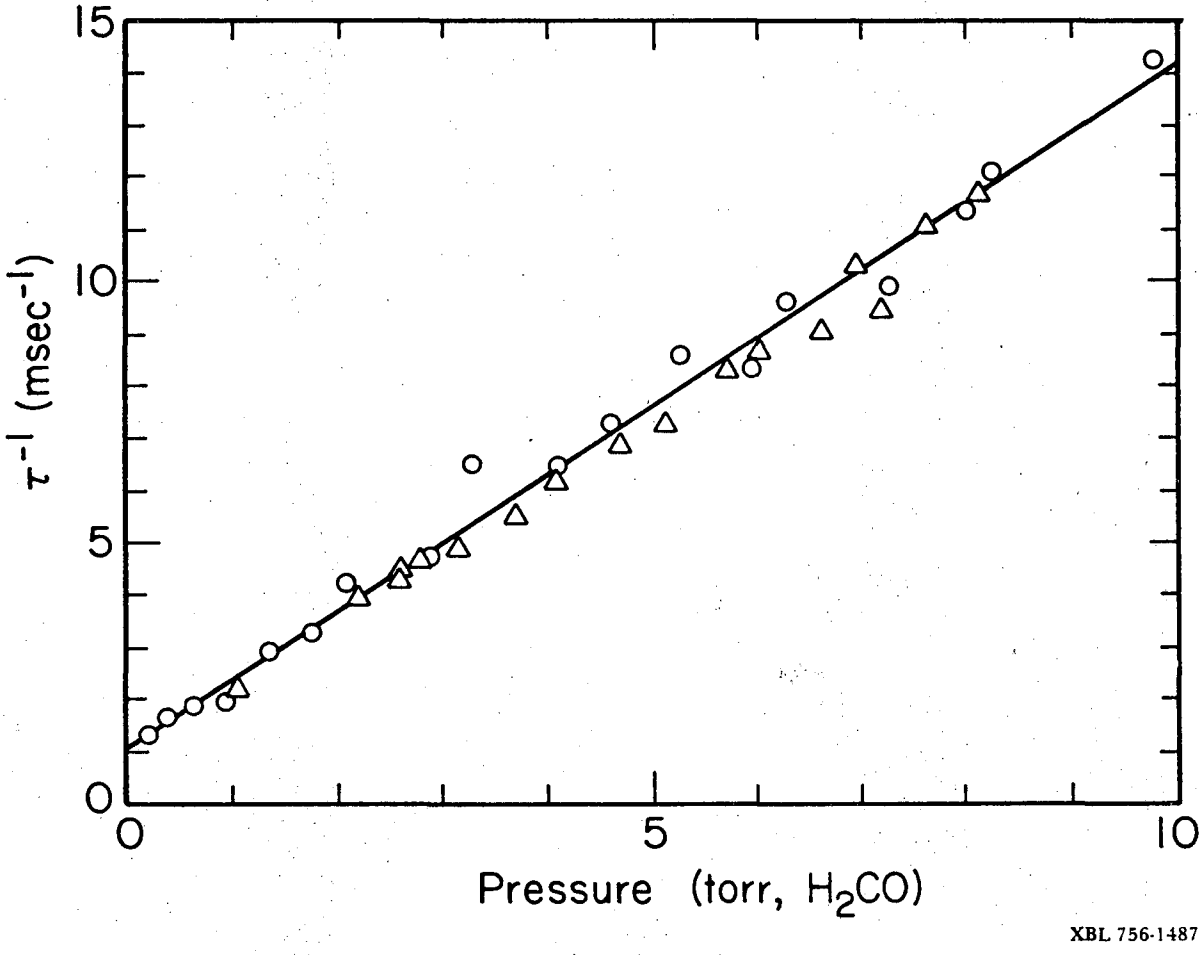

Fig. 7

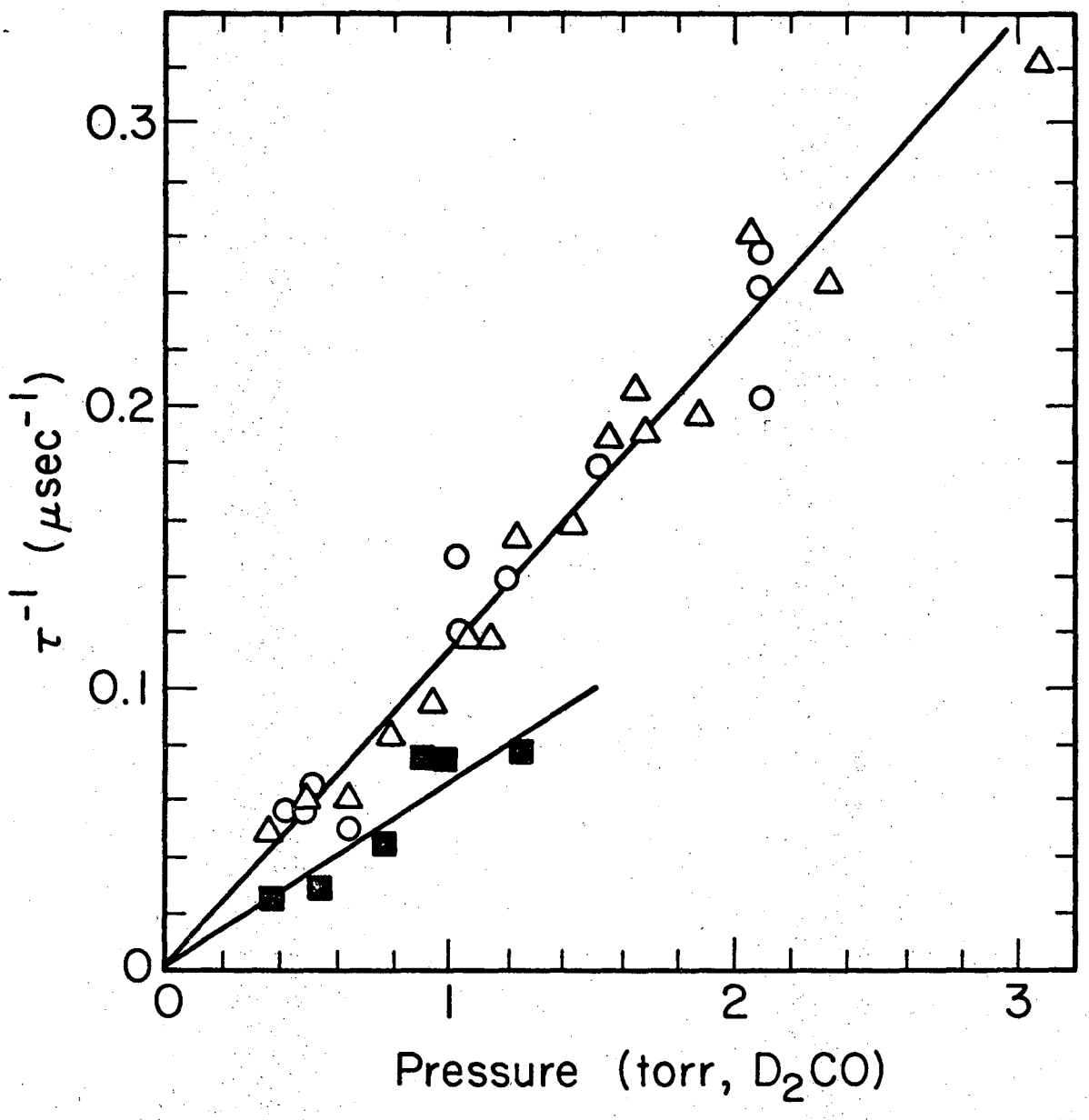

XBL 756-1482

Fig. 8

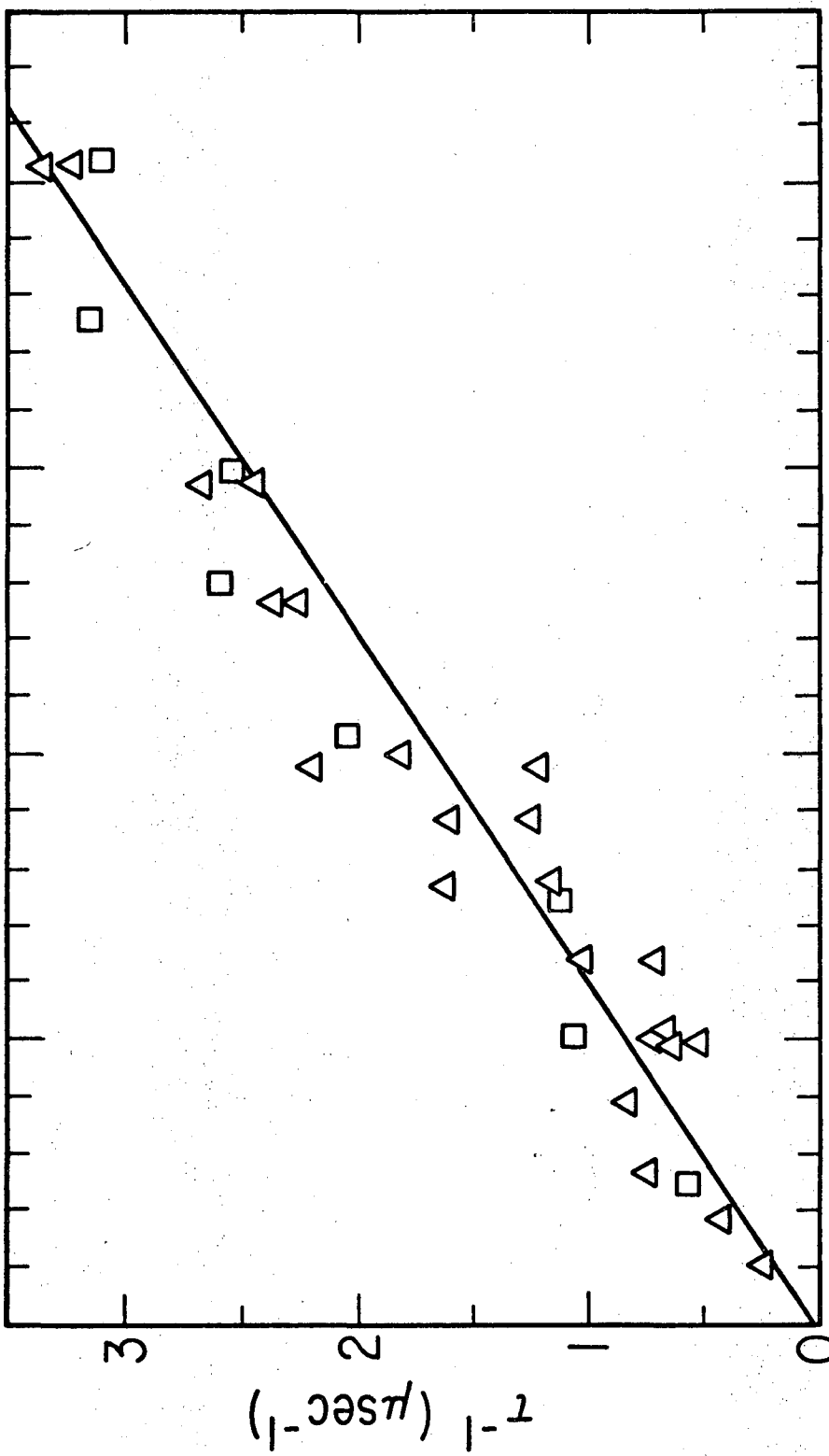

XBL 755-1437

Fig. 9a

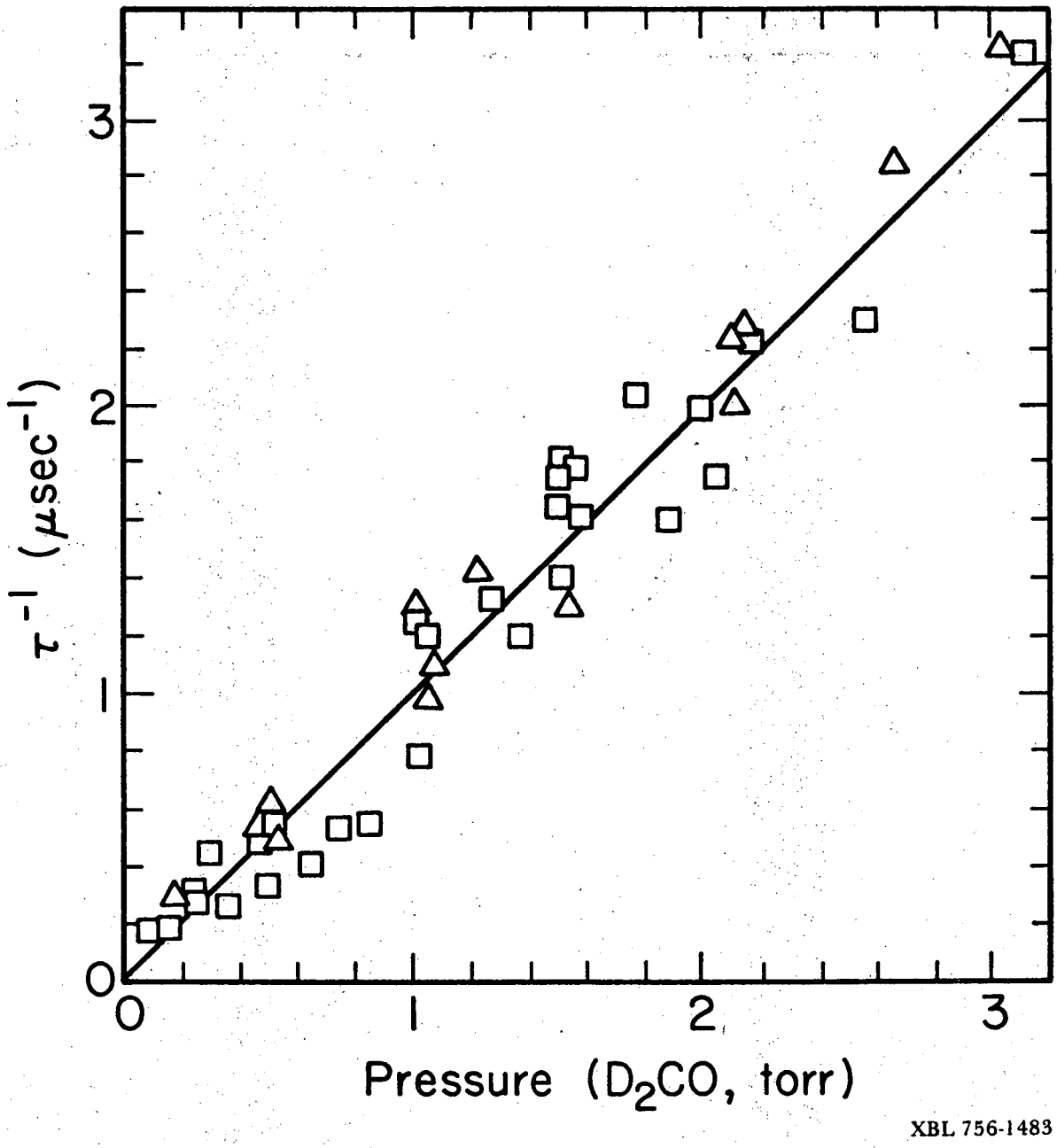

Fig. 9b

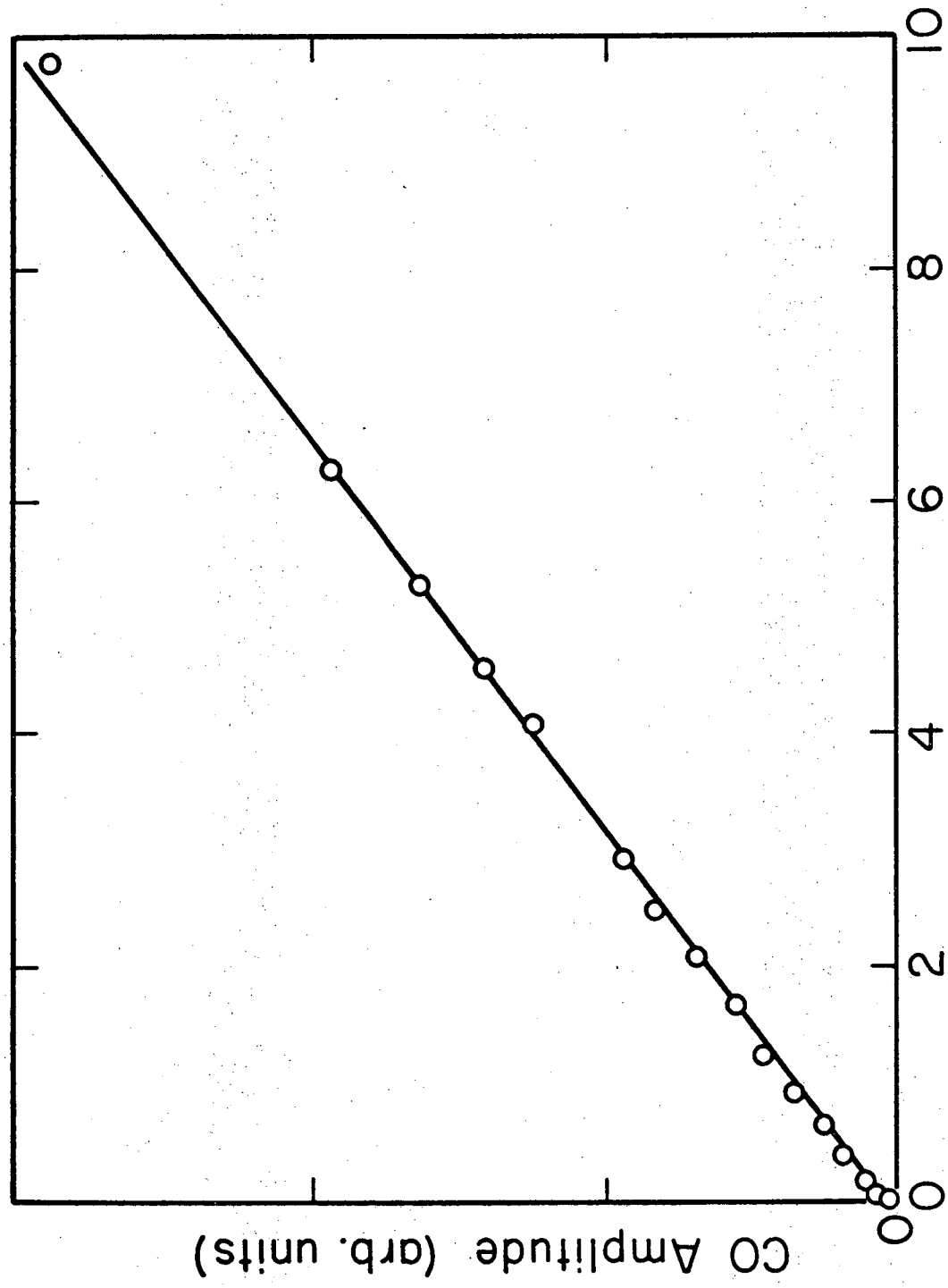

XBL 756-1485

Fig. 10

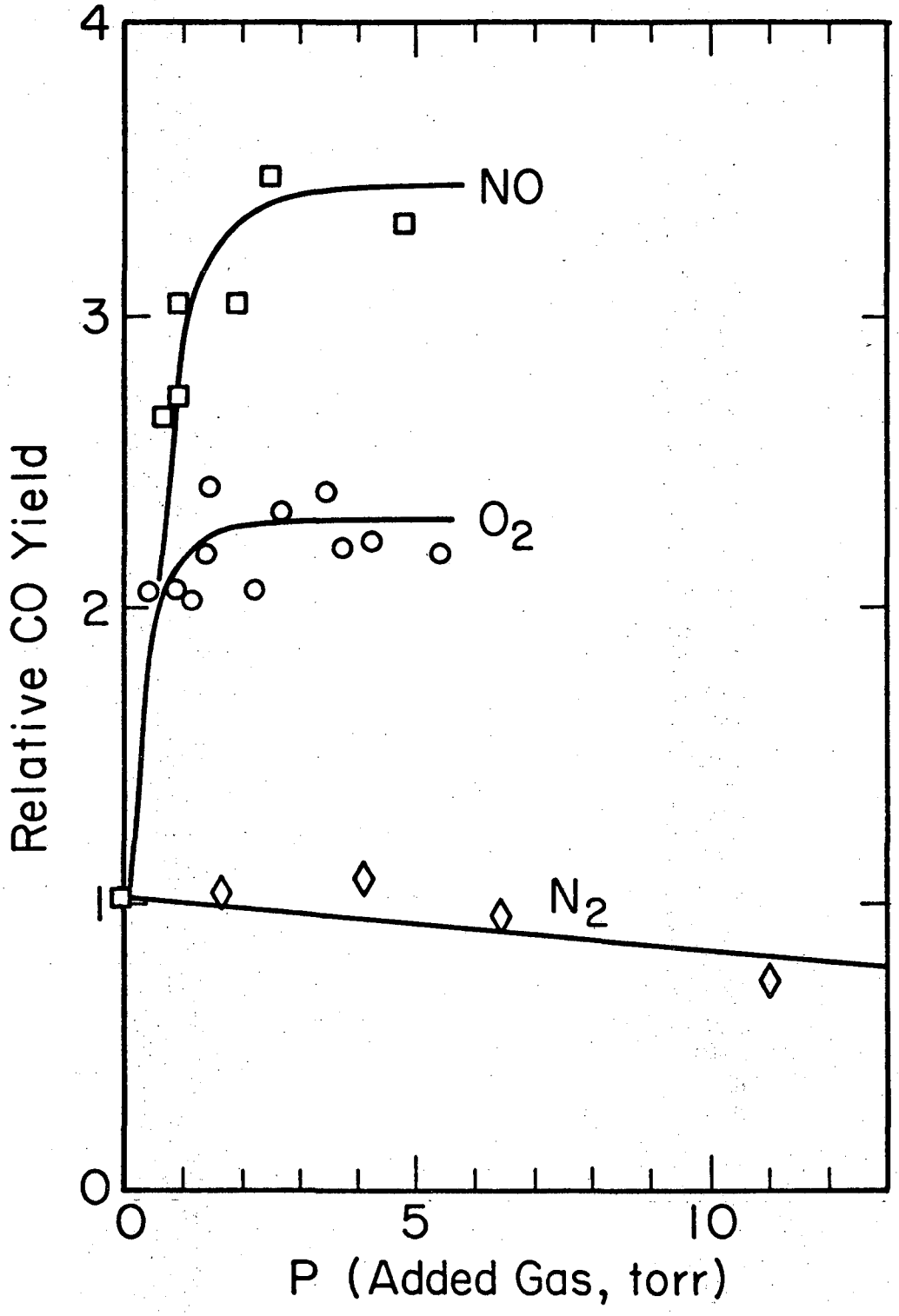

XBL 756-1484

Fig. 11

TECHNICAL INFORMATION DIVISION
LAWRENCE BERKELEY LABORATORY
UNIVERSITY OF CALIFORNIA
BERKELEY, CALIFORNIA 94720